BRITISH ANTARCTIC SURVEY

(formerly Falkland Islands Dependencies Survey)

SCIENTIFIC REPORTS

No. 46

GEOPHYSICAL INVESTIGATION OF THE SCOTIA ARC

By

D. H. GRIFFITHS, M.Sc., Ph.D., R. P. RIDDIHOUGH, M.Sc.,

Department of Geology, University of Birmingham

H. A. D. CAMERON *and* P. KENNETT, M.Sc.

British Antarctic Survey
and
Department of Geology, University of Birmingham

LONDON: PUBLISHED BY THE BRITISH ANTARCTIC SURVEY: 1964

BRITISH ANTARCTIC SURVEY SCIENTIFIC REPORTS: No. 46

GEOPHYSICAL INVESTIGATION OF THE SCOTIA ARC

By

D. H. GRIFFITHS, M.Sc., Ph.D., R. P. RIDDIHOUGH, M.Sc.,
Department of Geology, University of Birmingham

H. A. D. CAMERON *and* P. KENNETT, M.Sc.
British Antarctic Survey
and
Department of Geology, University of Birmingham

(Manuscript received 14th November, 1963)

ABSTRACT

DURING the four Antarctic summer seasons 1959–60 to 1962–63 investigations were carried out in the Scotia Sea, Bransfield Strait and adjacent areas. A network of gravity stations has been established in the Falkland Islands Dependencies and British Antarctic Territory, and connected through Port Stanley in the Falkland Islands to a station at Buenos Aires (Ezeiza international airport) at which the absolute value of gravity is known. In all about 150 gravity stations have been measured, and from these measurements a Bouguer anomaly map of the South Shetland Islands and northern Graham Land has been prepared. The most interesting feature of the map is the sharp elongated high of about +130 mgal centred over the South Shetland Islands. This feature seems to be associated with a marked magnetic high off the north coast of these islands. The gravity and magnetic highs are believed to be caused by faulting which has uplifted a high-density crustal layer beneath the islands. This layer, which has a seismic velocity of 7·4 km./sec., is known from refraction measurements to be at a depth of about 8 km. in Bransfield Strait.

About 15,000 nautical miles (28,000 km.) of total field magnetic profile have been obtained in crossings of the Scotia Sea and the Scotia Ridge. In general the traverses are too far apart for any contouring to be possible, or even for magnetic trends to be recognized. For this reason an attempt has been made to develop a statistical method of dealing with these data. In relatively well surveyed regions this method has made it possible to delineate areas of different magnetic type which it is thought may be related to the geological structure of the sea floor. In one of these areas the magnetic anomalies are interpreted as being due to bodies with their top surfaces at a relatively constant but shallow depth beneath the ocean floor. It is believed that the magnetic features arise from either steep-sided intrusions or are due to topographic relief of a basic crust.

A number of seismic refraction profiles have been surveyed in Bransfield Strait and the Scotia Sea between the South Orkney Islands and South Georgia. A preliminary interpretation indicates the main crustal layer north of the South Orkney Islands trench has a velocity of about 6 km./sec., suggesting that it is not truly oceanic in character.

CONTENTS

I. INTRODUCTION

IN 1959 the Falkland Islands Dependencies Survey agreed to collaborate with the geophysics section of the Department of Geology, University of Birmingham, by providing facilities for carrying out geophysical surveys in those regions of Antarctica and the surrounding waters in which they operated. The aim of the proposed investigations was to obtain information about the nature and structure of the Earth's crust and upper mantle in this region, particularly in the Scotia Sea and across the Scotia arc* (Griffiths, 1963). The latter is the name given to the great loop of islands and submarine ridges which apparently forms a structural connection between South America and the narrow mountainous peninsula of Graham Land. The structure has many features in common with other island arcs, the general characteristics of which have been discussed, among others, by J. Tuzo Wilson (1954).

1. *Geology*

General accounts of the geology of the Scotia Ridge have been given by Holtedahl (1929), Barth and Holmsen (1939), Tyrrell (1945), Adie (1957*a*, 1957*b*, 1958, 1962, 1964), Matthews (1959) and Hawkes (1962). Detailed descriptions of certain areas are given in the *Falkland Islands Dependencies Survey* and *British Antarctic Survey Scientific Reports*. The main geological facts relevant to the geophysical investigations are given below.

At the present time the active area of the Scotia arc is the South Sandwich Islands. This island group is typical of island arcs in that it has an arcuate form, is composed entirely of volcanic rocks and has a deep trench on its convex side. The geology of the other parts of the arc is more complex, since they are much older. A metamorphic Basement Complex of (?) Precambrian age is known from southern Graham Land, and a substantial thickness of *para*-schists representing regionally metamorphosed argillo-arenaceous and calc-argillaceous sediments occurs in the South Orkney Islands. Thick successions of greywacke-facies sediments of possible Carboniferous age are present in the northern part of Graham Land, in the South Orkney Islands and South Georgia, and in late Palaeozoic times there was probably already in existence a continuous geosyncline through the Scotia arc from the South American Andes to Graham Land. The most important phase which took place during the Upper Jurassic was a period of great vulcanicity in Graham Land and the South Shetland Islands.

During the Cretaceous the Magellan geosyncline developed adjacent to the late Palaeozoic trough, though it should be noted that the Cretaceous conglomerates recorded from the South Orkney Islands are of shallow-water origin. It was not until the late Cretaceous to early Tertiary that western Antarctica and Graham Land achieved much of its present elevation. Folding and uplift was accompanied by large-scale intrusion of the Andean Intrusive Suite batholiths. Volcanic activity recurred in the Miocene in the South Shetland Islands and off the north-east of Graham Land along arcuate lines parallel to the belt of Andean intrusions, and this has continued sporadically in the former area until recent times. The South Shetland Islands are fronted by an oceanic trench and appear to represent the latest stage of island arc formation in this area.

The geological history of this region is not yet completely understood, but some interesting contributions have been advanced by Matthews (1959) and Hawkes (1962). Matthews has discussed the similarities and differences between the Scotia arc and the Caribbean Arc. The latter has been intensively studied by Officer and others (1959), using mainly seismic refraction techniques. They have found that in the Venezuelan basin the structure of the crust is significantly different from that of the open ocean, and that there are two high-velocity layers present; the total thickness is somewhat greater than the 5 km. of normal high-velocity crust. Beneath Puerto Rico the crustal thickness calculated from the gravity and seismic data is about 20 km. The explanation given for the origin of the arc is that the entire area of the Caribbean has been extensively intruded by a differentiate migrating upwards from deep in the mantle, and that the islands and ridges are the areas where most of this differentiate reached the surface. As a result of the extensive intrusion the Caribbean sea floor, now no longer oceanic in character, expanded and was overthrust on to the oceanic crust, thus creating a deep trench on the convex side of the arc. Whether this explanation is compatible with the results of the recent seismic work in the trench described by Bunce and Fahlquist (1962) is not at present clear. Matthews (1959) has argued, however,

* The designation "Scotia arc" is used throughout this report to describe the arcs of ridges *and troughs* in the Scotia Sea area. It is not to be regarded as a place-name but is a concept based on geophysical evidence. It is not synonymous with the place-name "Scotia Ridge" which refers only to the main ridge.

that in the Scotia arc the process is the reverse of that advanced to explain the origin of the Caribbean Arc and that a continental mass of considerable size has sunk within the area of the Scotia Sea. This must now be in the process of being turned into an oceanic crust but the submergence and continued existence of so large a sialic region is difficult to conceive as possible. This argument is supported by discussion of the above-mentioned geological facts, such as the occurrence of basement rocks and shallow-water deposits in the South Orkney Islands and the source of the sediments in South Georgia.

Hawkes (1962) has suggested that the islands of the Scotia Arc, excluding the South Sandwich Islands, are fragments of a former sialic bridge between South America and Antarctica which was disrupted in post-Carboniferous but pre-Jurassic times; the fragments subsequently drifted eastwards as a result of the advance of the Pacific crust, presumably by convection in the mantle. The bathymetric chart gives little support to this idea, for there appears to be an almost continuous ridge from South America, through the various island groups of the arc, to Graham Land. Moreover, the evidence from rock magnetism investigations strongly supports the view that South America and Antarctica drifted nearer together during late Mesozoic times (Blundell and Stephenson, 1959). Hawkes has also suggested that the volcanically active South Sandwich Islands constitute a new arc built out to the east of the original structure. If this is correct, it might be possible to detect by geophysical methods the remnants of the older arc joining South Georgia to the South Orkney Islands, now no longer apparent even as a submarine ridge.

2. *Other geophysical work in the area*

The results of some geophysical work in this area have already been described. Gravity values at a number of Chilean bases have been reported by Cohen (1963). Gravity measurements have also been made at a number of Argentine stations and at other points by the Instituto Geografico Militar (1957–58). These results have been privately circulated but they have not been published. J. and M. Ewing (1959) have also reported the results of 74 seismic refraction profiles made in 1958 and 1959 by *Vema* and the Argentine naval oceanographic vessel *Sanaviron* (Woollard, 1960).

3. *Survey organization*

Circumstances were such that for the first two seasons (1959–60 and 1960–61) only magnetic measurements at sea and land gravity measurements could be made. In the 1961–62 season a start was made with seismic work, and several short lines were shot in Bransfield Strait. During the 1962–63 season, using improved equipment, a number of long seismic lines were surveyed on a track from the South Orkney Islands to South Georgia, and the magnetic and gravity measurements were continued.

The first season's (1959–60) field work was done by D. H. Griffiths,* but in the two following seasons (1960–61 and 1961–62) it was undertaken by H. A. D. Cameron*† and P. Kennett.† M. J. G. Cox† assisted with the seismic work during the 1961–62 season and A. Allen† during the 1962–63 season. The group was joined by E. Parkinson* in 1962. R. P. Riddihough* has been mainly concerned with the interpretation of the magnetic data.

For the first three seasons (1959–60, 1960–61 and 1961–62) the cost of the field work was borne mainly by the British Antarctic Survey, but since October 1962 the investigation has been financed by a grant from the Department of Scientific and Industrial Research to the geophysics section of the Department of Geology, University of Birmingham. This does not, however, cover the cost of running the ships, which is still the responsibility of the British Antarctic Survey. With the exception of the first season (1959–60) when some gravity measurements were made with the assistance of R.R.S. *John Biscoe*, all the geophysical work has been done with R.R.S. *Shackleton*. Valuable assistance with the seismic operations has been given by H.M.S. *Protector*, and all explosive has been supplied by the Admiralty.

II. THE GRAVITY SURVEY

1. *Instruments*

Two Worden gravimeters were used for the survey, No. 14 during the first season (1959–60) and No. 556 subsequently. Instrument No. 14 was kindly loaned by Professor G. P. Woollard of the University of Wisconsin. Being an early model it has no thermostat and also it is not fitted with a geodetic dial.

* Department of Geology, University of Birmingham.
† British Antarctic Survey.

The latter disadvantage was somewhat offset by the fact that the small dial of the instrument has a range of 1,000 mgal, which was adequate for all the measurements, with the exception of the gravity difference between Montevideo and the Falkland Islands. Since the only way of making an independent connection between the Antarctic network of gravity stations and the world network was by means of this link the absence of the geodetic dial was a serious limitation. In an attempt to overcome this the geodetic dial belonging to the Worden gravimeter of the Department of Geology, University of Birmingham, was fitted to instrument No. 14 and used to measure the large gravity differences. The calibration was kindly done for us by the makers when the instrument was returned to the United States after the first season's work. The calibration showed that the instrument was satisfactory for use over the full geodetic dial range, and the measurement made of the Montevideo to Port Stanley gravity difference carried out during the 1959–60 season is therefore acceptable.

Worden No. 556, which is the property of the British Antarctic Survey, was used in subsequent seasons (1960–63). It has a geodetic dial and thermostatically controlled temperature stabilization.

On all occasions at sea the instruments were slung by elastic ropes on the ship's after-deck in order to minimize shock and vibration due to movements of the vessel, and also to avoid sudden changes in ambient temperature, such as would have resulted had they been taken inside the ship after each reading. All landings were made by motor boat or dinghy, during which time the instruments were carried by the operators.

2. *Calibration*

The small dial constant of No. 14, as supplied by Professor Woollard, was 0·12581 mgal/scale division. A tilt-table determination by Texas Instruments Ltd., carried out after the 1959–60 season, gave a figure of 0·12603 mgal/scale division. This latter value was used in calculating all major links in which the small dial was used, since the calibration was done immediately after the survey, but even if Professor Woollard's value was correct the maximum errors in the gravity differences due to this are only about 0·1 mgal, which is commensurate with other measuring errors. The geodetic dial, calibrated after the survey, was used only in the measurement of the link between Port Stanley and Montevideo.

Table I gives the values of the calibration constant of Worden No. 556 as determined on successive occasions. The first value (August 1960; at 83° F) is the makers' tilt-table calibration. The other values

TABLE I

CALIBRATION FACTORS FOR WORDEN GRAVIMETER NO. 556 AT VARIOUS TEMPERATURES
(in mgal/scale division)

Date	*Temperature* (° F)					
	86°	83°	80°	63°	57°	47°
August 1960		0·22950		0·22916	0·22910	0·22892
September 1960		0·22950				
June 1961	0·22970					
June 1962			0·22940			

were determined from measurements against H.M. Geological Survey's base line in Derbyshire. Calibration factors for the temperatures at which the instrument was maintained in the Antarctic (63°, 57° and 47° F) were taken from the graph supplied by the makers. These factors are given in the last three columns of the top line of Table I and they are based on the makers' tilt-table determination made at 83° F. Our three determinations agree almost exactly with the makers' figure when corrected to 83° F, indicating, rather surprisingly, a constant value for the calibration factor. The makers' calibration was accepted for the geodetic dial. It has since been checked against the small dial with satisfactory agreement, but unfortunately it has not been possible to calibrate the instrument over a long base line.

3. *Survey procedure*

All gravimeters are subject to a drift of the scale reading, arising mainly from creep in the main spring. The drift rate in some instruments appears to be affected by temperature, and there is evidence from our work that the mode of transport is also important. This means that any measured difference will be in error by the amount of drift that has taken place in the period between the two readings. Provided the instrument is not subjected to rapid changes of temperature or to violent motion during transport the drift rate may be assumed to be approximately linear, and a correction can be applied to any difference measurements made. It is best determined by repeating readings at a particular station during the course of a survey. Unfortunately, during a survey of the type being described it was sometimes not possible to re-occupy any of the stations measured until after an interval of days or even weeks. When this occurred somewhat different procedures were adopted to determine the drift rate. For example, it was not uncommon for the difference between two stations A and B to be measured on the outward voyage, the difference B to A being determined on the return some weeks later. When this happened a correction was made for the amount of drift that had taken place in the period between the two measurements at B, and the readings were then treated as a single closed loop ABA. As the time taken in travelling between A and B and back to A was rarely more than a week it was possible, from these measurements, to get a reasonably satisfactory average drift rate for the period and so make the necessary correction to the measured A to B difference. In practice, the drift rates so determined often did not differ significantly from the average drift rate for the whole voyage but sometimes, after rough sea voyages, there were differences.

Another method of checking drift was also used. Whenever a stop of 24 hr. or more was made the gravimeter was set up and read at convenient intervals; from these readings a drift rate was calculated. The drift rate during the working periods was then interpolated from the values thus found. This method was satisfactory so long as the ship was working in sheltered waters, because in such circumstances the drift rate remained fairly constant. After a rough voyage it was usually found to have altered, though it returned to its normal value within a day (this was so for both instruments). In these circumstances it was better to use an average drift rate for the voyage, and this was determined by one of the other methods already described. The periods over which the average drift rates were determined varied between a few days and about ten. During these periods it was occasionally, though not often, possible to use a short stop to make a check determination. Thus, for relatively long periods there was no way of checking for local fluctuations in drift rate or sudden jumps in the drift, and it is obvious from a comparison of repeated measurements that the gravity differences measured between stations separated by several hundred miles of open sea are subject to much larger errors than are usual in land surveying.

Gravity measurements were made at all British Antarctic Survey scientific stations visited during the course of the survey. Most of these were visited on several occasions, thus making possible a number of determinations of the gravity differences between them. Fig. 1 shows the network of stations established. The averages of the measured gravity differences between stations are given, together with their standard errors. The average gravity differences were obtained by correcting each one-way determination, using the appropriate average drift rate, and then taking the mean. Since the standard errors are each based only on four to six measurements they must be regarded merely as rough estimates.

When a gravity difference, such as that between Port Stanley and Signy Island, has been measured by two different routes, for example, by way of South Georgia and also via Deception Island, the two measurements of the difference should agree. Any discrepancy is likely to be due mainly to uncorrected instrument drift. This is known as the "closure error" of the loop and it has to be distributed among all the measurements, the resulting values being the best values of the gravity differences that can be obtained from the data. The closure errors of the triangle and the quadrilateral are given in Fig. 1. That of the quadrilateral is surprisingly large when compared with the standard error of the individual links, but careful study of the data has not revealed any special reason which might account for it. The polygon was therefore adjusted to give zero closure, the individual links being weighted in inverse proportion to the size of their standard errors.

Fig. 2 shows the complete network of base stations, including the adjusted link. Where no standard error is quoted too few measurements have been made for any useful estimate to be calculated, but with the exception of the link to Zavodovski Island (which might be in error by one or two milligals) these differences are believed to be correct to within a few tenths of a milligal, for they are links involving

only short sea passages or air flights. Thus, within the Dependencies, apart from the exception quoted, it seems very probable that a few tenths of a milligal can be taken as the accuracy of the survey.

Before true gravity values can be assigned to a network of stations, the network has to be linked to a point at which the absolute value of gravity is known. The most convenient reference point in this instance is Ezeiza international airport at Buenos Aires, a point which is well connected to the international network of gravity stations. The values adopted for the measured differences between Buenos Aires and the Dependencies are also shown in Fig. 2. These are provisional because, for one thing, the scale factors of the two gravimeters were obtained by tilt-table calibration, and secondly it is doubtful whether it is possible to obtain a very accurate value of the difference using a Worden gravimeter, even after repeating the measurements several times. An instrument with a much lower drift rate which is less affected by mode of transport is necessary.

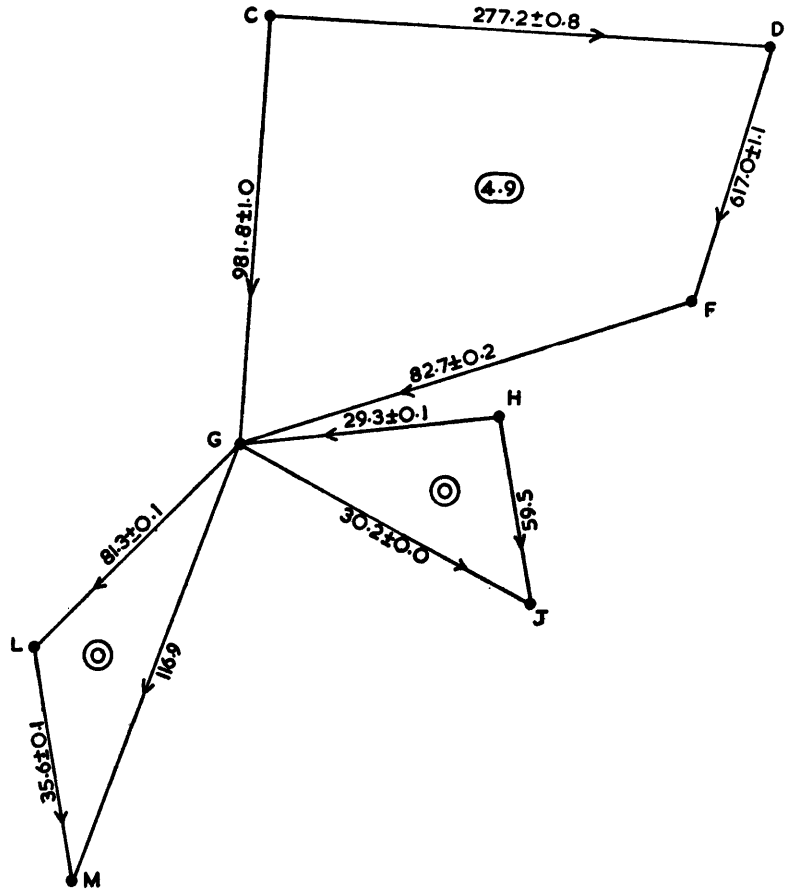

FIGURE 1

Network of gravity base stations in the Falkland Islands, Falkland Islands Dependencies and British Antarctic Territory, and closure errors. Station differences are given in mgal. For the key to letters see the caption to Fig. 2.

For comparison, the absolute values of gravity finally adopted for the stations at Port Stanley, Deception Island, Signy Island and Port Lockroy, together with values directly derived from the Argentinian gravity network, are given in Table II. These were obtained by means of single short links between the British Antarctic Survey scientific stations and the nearest Argentinian stations, mainly those at Deception Island, Laurie Island and the Melchior Islands. As mentioned previously, gravity measurements had been made at these points by the Instituto Geografico Militar, the absolute values being based on relative pendulum measurements made at "Esperanza" (Hope Bay). By means of a link with the British Antarctic Survey station at Hope Bay a comparison can be made with the gravity value at "Esperanza". It is evident that there is a difference of 11 mgal between the two readings. At the other three Argentinian stations it was not possible to identify the exact location of their gravity observation stations, but altitude

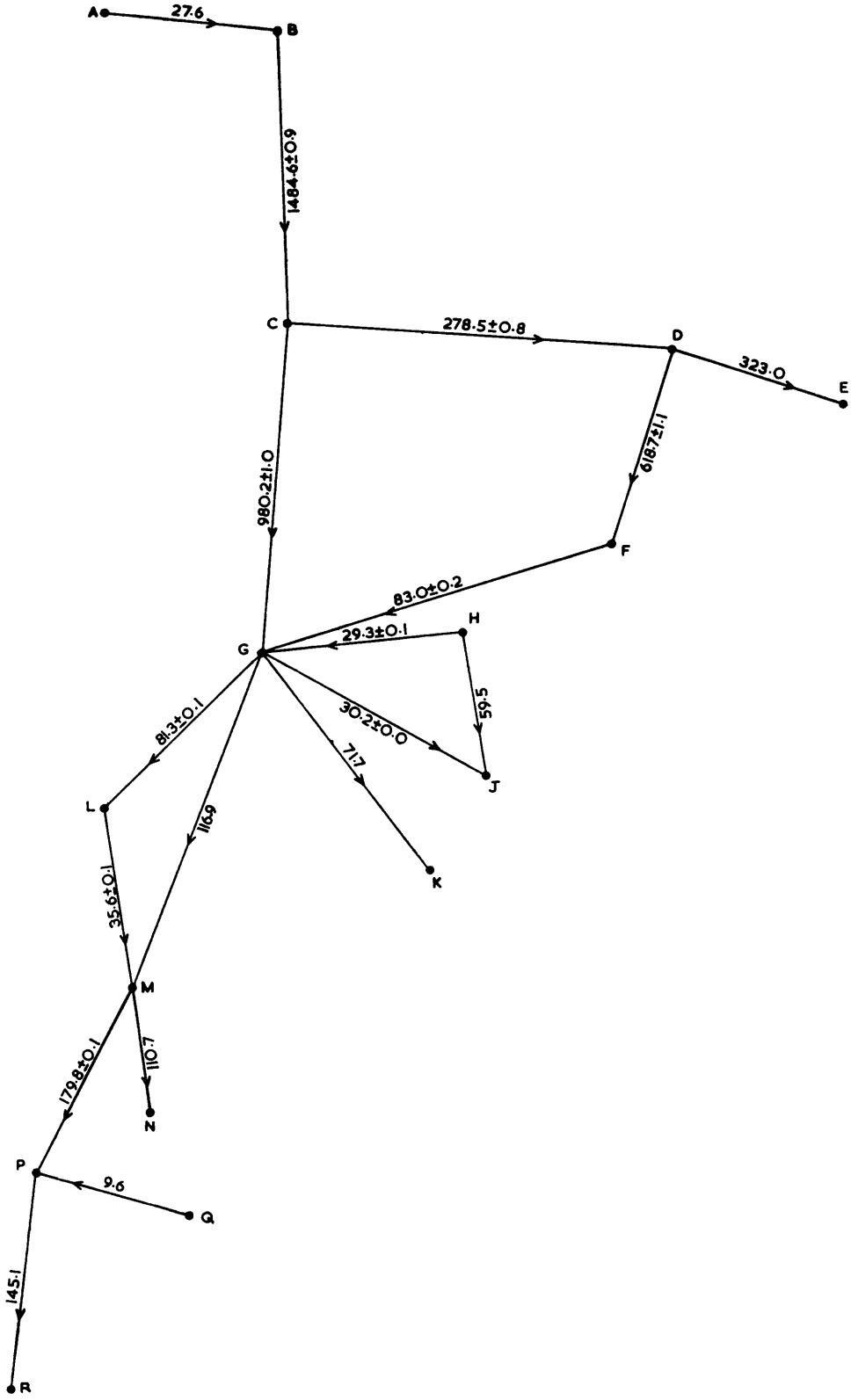

FIGURE 2

Network of gravity base stations in South America, the Falkland Islands, Falkland Islands Dependencies and British Antarctic Territory. Station differences are given in mgal.

A	Buenos Aires.	E	Zavodovski Island.	J	Hope Bay.	N	Detaille Island.
B	Montevideo.	F	Signy Island.	K	North of Cape Longing.	P	Adelaide Island.
C	Port Stanley.	G	Deception Island.	L	Port Lockroy.	Q	Stonington Island.
D	South Georgia.	H	Admiralty Bay.	M	Galindez Island.	R	Fossil Bluff.

TABLE IIA

COMPARISON OF GRAVITY BASES

(Gravity values in cm. sec.$^{-2}$)

Locality	*British Antarctic Survey*	*U.S. Glacier, 1960*	*Argentina, 1957–58*	*Cohen, 1963*
Buenos Aires (Ezeiza airport)	979·7330	979·7320*		
Montevideo	979·7606			
Port Stanley	981·2452	981·2405		
Deception Island	982·2254	982·2195	982·2137	982·2258†
Signy Island	982·1424		982·1320	
Port Lockroy	982·3067		982·2942	
Argentine pendulum station at Hope Bay ("Esperanza")	982·2546		982·2433	

* Different reference point to that used by British Antarctic Survey.
† Based on the gravity station at Punta Arenas.

TABLE IIB

COMPARISON OF GRAVITY STATIONS

(Gravity values in cm. sec.$^{-2}$)

Locality	*Latitude* (S.)	*Longitude* (W.)	*British Antarctic Survey*	*Cohen, 1963*
Waterboat Point (Chilean pendulum station)	64°49·2′	62°51·6′	982·3075	
"General González Videla"				982·3080†
South Bay, Doumer Island*	64°52·4′	63°34·2′	982·3187	
"French Cove"‡	64°53′	63°34′		982·3174†

* The distance between these two stations is estimated as less than 400 yd. (366 m.). The correction has been applied for altitude.
† Based on the gravity station at Puntas Arenas.
‡ "Caleta French" on Argentine chart 129 (1957 edition).

differences between our stations and others can account for only a few tenths of a milligal of the discrepancies in the two sets of observations, which are again of the order of 10 mgal.

An error in the Argentinian pendulum observations is suggested by the fact that there is only 0·5 mgal difference between our value at the British Antarctic Survey station at Deception Island and that obtained by Cohen (1963), although the single "one-way" determination by U.S. *Glacier* (Operation "Deep-Freeze", 1960) gives a value at this base which lies between our value and that of the Argentinians. It is also surprising that, even when the possibility of errors due to differences in station positions is taken into account, the differences between the Argentinian and British Antarctic Survey values vary by as much as 2·1 mgal. These differences are far greater than the standard errors of our observations. A complete list of values at the British Antarctic Survey gravity stations is given in Table III. Exact station localities at all the gravity bases are shown in Figs. 3–18.

4. *Reduction of the observations*

The preparation of the Bouguer anomaly map necessitates making several corrections to the observed gravity values. They must be adjusted to a common reference level, normally sea-level, and corrected for the variation of gravity with latitude. The latter is obtained from tables calculated from the

TABLE III

GRAVITY VALUES MEASURED DURING 1959–62

(Gravity base stations indicated with an asterisk)

Locality	*Latitude* (S.)	*Longitude* (W.)	*Height* (m.)	*Height Correction* (mgal)	*Theoretical Gravity at This Latitude* (cm. sec.$^{-2}$)	*Absolute Value of Gravity* (cm. sec.$^{-2}$)	*Bouguer Anomaly* (mgal)
*PORT STANLEY	51°41·5′	57°51·1′	—	0	981·2283	981·2452	+16·9
SOUTH GEORGIA							
Bird Island	54°00·5′	38°03·1′	—	0	981·4298	981·5560	+126·2
Elsehul	54°01·5′	37°58·0′	—	0	·4312	·5550	+123·8
Right Whale Bay	54°00·0′	37°42·0′	—	0	·4291	·5345	+105·4
Wales Head	54°00·9′	37°34·5′	—	0	·4312	·5274	+96·2
Rosita Harbour	54°01·0′	37°28·0′	—	0	·4305	·5103	+79·8
Lighthouse Bay	54°03·0′	37°08·8′	—	0	·4334	·5047	+71·3
Leith Harbour	54°08·0′	36°41·5′	—	0	·4406	·5042	+63·6
Stromness	54°09·4′	36°42·6′	—	0	·4426	·5036	+61·0
Husvik	54°10·6′	36°42·6′	—	0	·4443	·5093	+65·0
*King Edward Point	54°16·5′	36°29·5′	—	0	981·4527	981·5237	+71·0
Moraine Fjord	54°19·4′	36°29·4′	—	0	·4569	·5255	+68·6
Godthul	54°17·7′	36°17·0′	—	0	·4545	·5237	+69·2
Royal Bay	54°31·0′	36°04·1′	—	0	·4734	·5684	+95·0
Gold Harbour	54°36·7′	35°56·0′	—	0	·4813	·5818	+100·5
Larsen Harbour	54°50·3′	36°00·0′	—	0	·5007	·6595	+158·8
Undine South Harbour	54°30·8′	36°36·1′	—	0	·4731	·5996	+126·5
Clerke Rocks	55°02·0′	34°38·0′	—	0	·5174	·7131	+195·7
SOUTH SANDWICH ISLANDS							
*Zavodovski Island	56°16·3′	27°33·6′	4	+0·7	981·6217	981·8467	+225·7
Leskov Island	56°40·0′	28°10·0′	—	0	·6546	·8390	+184·4
Visokoi Island	56°40·8′	27°12·6′	4	+0·7	·6558	·8499	+194·8
Candlemas Island	57°04·0′	26°44·0′	—	0	·6877	·8877	+200·0
Vindication Island (1)	57°06·0′	26°47·0′	4	+0·7	·6905	·8975	+207·7
Vindication Island (2)	57°06·5′	26°46·2′	4	+0·7	·6912	·8983	+207·8
SOUTH ORKNEY ISLANDS							
Cape Geddes	60°42·2′	44°35·0′	—	0	981·9787	982·1490	+170·3
Cape Mabel	60°41·3′	44°40·3′	—	0	·9775	·1491	+171·6
North-west of Cape Dundas	60°43·2′	44°26·7′	—	0	·9799	·1532	+173·3
Scotia Bay	60°45·0′	44°43·0′	5	+1·0	·9822	·1549	+173·7
Murray Islands	60°47·2′	44°31·0′	—	0	·9851	·1505	+165·4
Fredriksen Island	60°44·9′	44°59·0′	—	0	·9821	·1506	+168·5
Gibbon Bay	60°39·0′	45°12·7′	—	0	·9745	·1433	+168·8
Coffer Island	60°46·0′	45°08·5′	3	+0·6	·9835	·1423	+159·4
Sandefjord Bay	60°36·7′	46°01·9′	—	0	·9715	·1511	+179·6
Pantomime Point	60°44·3′	45°34·8′	—	0	·9812	·1417	+160·5
*Signy Island	60°43·0′	45°35·6′	4	+0·7	981·9795	982·1422	+163·4
SOUTH SHETLAND ISLANDS							
Point Wild	61°03·0′	54°48·0′	—	0	982·0053	982·1124	+107·1
Elephant Island	61°07·0′	54°49·0′	—	0	·0104	·1169	+106·5
Rowett Island	61°15·0′	55°09·0′	—	0	·0206	·1750	+154·4
Gibbs Island	61°28·0′	55°24·0′	—	0	·0371	·2191	+182·0
North Foreland	61°53·0′	57°40·0′	—	0	·0686	·1711	+102·5
Cape Melville	62°02·0′	57°35·0′	—	0	·0798	·1807	+100·9
Penguin Island	62°06·0′	57°56·0′	—	0	·0848	·1907	+105·9
Owen Island	61°55·0′	58°21·0′	—	0	·0711	·1838	+112·7
Lussich Cove	62°05·7′	58°20·6′	—	0	·0844	·1952	+110·8
*Admiralty Bay	60°05·0′	58°24·5′	9	+1·8	982·0836	982·1961	+114·3
Ardley Island	62°13·0′	58°57·0′	—	0	·0936	·2257	+132·1
Nelson Island	62°21·0′	59°08·0′	—	0	·1035	·2348	+131·3
Robert Point	62°27·0′	59°24·0′	—	0	·1109	·2362	+125·3
Coppermine Cove	62°23·0′	59°42·4′	—	0	·1060	·2153	+109·3
Fort William	62°26·5′	59°43·3′	—	0	·1103	·2219	+111·6
Renier Point	62°37·0′	59°51·0′	4	+0·7	·1233	·2481	+125·5
Edinburgh Hill	62°33·0′	60°03·0′	—	0	·1183	·2352	+116·9
Elephant Point	62°42·0′	60°26·0′	—	0	·1294	·2294	+100·0
South-west Livingston Island	62°41·0′	60°50·0′	—	0	·1282	·2524	+124·2

TABLE III (*continued*)

Locality	*Latitude* (S.)	*Longitude* (W.)	*Height* (m.)	*Height Correction* (mgal)	*Theoretical Gravity at This Latitude* (cm. sec.$^{-2}$)	*Absolute Value of Gravity* (cm. sec.$^{-2}$)	*Bouguer Anomaly* (mgal)
SOUTH SHETLAND ISLANDS (*cont.*)							
Cape Shirreff	62°28·0′	60°49·0′	—	0	·1122	·2200	+107·8
*Deception Island	62°58·9′	60°34·1′	—	0	982·1502	982·2254	+75·2
Chilean station, Deception Island	62°56·4′	60°36·0′	—	0	·1471	·2230	+75·9
Argentine station, Deception Island	62°58·8′	60°42·2′	9	+1·8	·1500	·2257	+77·5
Deception Island (1)	63°00·0′	60°34·5′	—	0	·1515	·2302	+78·7
Deception Island (2)	62°57·6′	60°36·3′	—	0	·1485	·2206	+72·1
GRAHAM LAND AND ISLANDS							
Danger Islands	63°25·0′	54°37·0′	—	0	982·1818	982·2633	+81·5
Etna Island	63°05·5′	55°10·7′	—	0	·1582	·2367	+78·5
Patella Island	63°07·5′	55°31·0′	—	0	·1606	·2343	+73·7
Wideopen Islands	63°00·5′	55°48·4′	—	0	·1521	·2230	+70·9
Paulet Island	63°34·2′	55°46·0′	—	0	·1930	·2519	+58·9
d'Urville Island	62°57·8′	56°26·0′	—	0	·1488	·2423	+93·5
Madder Cliffs	63°17·8′	56°29·0′	—	0	·1731	·2438	+70·7
Bransfield Island	63°11·9′	56°40·0′	—	0	·1660	·2445	+78·5
Jonassen Island	63°33·0′	56°43·0′	—	0	·1915	·2455	+54·0
Hope Island	63°02·6′	56°49·4′	—	0	·1546	·2343	+79·7
*Hope Bay	63°24·0′	56°58·6′	3	+0·6	982·1806	982·2556	+75·6
Cape Burd	63°39·0′	57°07·0′	—	0	·1987	·2511	+52·4
Gourdin Island	63°12·0′	57°17·0′	—	0	·1661	·2501	+84·0
Beak Island	63°39·0′	57°17·3′	—	0	·1987	·2468	+48·1
View Point	63°33·0′	57°21·0′	14	+2·7	·1915	·2528	+64·0
Eagle Island	63°38·0′	57°24·0′	—	0	·1975	·2490	+51·5
Crystal Hill	63°34·2′	57°49·0′	—	0	·1930	·2645	+71·5
Cape Legoupil	63°17·0′	57°52·0′	—	0	·1721	·2439	+71·8
Astrolabe Island	63°20·0′	58°36·0′	—	0	·1758	·2621	+86·3
Palmer Coast	63°31·0′	58°43·0′	—	0	·1891	·2698	+80·7
Cape Roquemaurel	63°33·0′	58°56·0′	—	0	·1915	·2630	+71·5
Blake Island	63°37·0′	59°03·0′	—	0	·1963	·2545	+58·2
Charcot Bay	63°48·0′	59°25·0′	—	0	·2095	·2689	+59·4
Almond Point	63°53·0′	59°33·0′	—	0	·2154	·2665	+51·1
Cape Kater	63°47·0′	59°55·0′	—	0	·2083	·2657	+57·4
Kendall Rocks	63°28·0′	59°45·0′	—	0	·1854	·2814	+96·0
Cape Wollaston	63°40·0′	60°47·6′	—	0	·1999	·2850	+85·1
Mikkelsen Harbour	63°54·0′	60°47·6′	—	0	·2166	·2838	+67·2
*8 miles north of Cape Longing	64°28·0′	59°00·0′	76	+14·9	982·2568	982·2971	+55·2
Hoseason Island	63°43·2′	61°39·0′	—	0	·2038	·2712	+67·4
Intercurrence Island	63°54·5′	61°24·0′	—	0	·2172	·2886	+71·4
Small Island	64°00·8′	61°27·7′	—	0	·2248	·2969	+72·1
North-east Liège Island	63°59·0′	61°49·5′	6	+1·2	·2226	·2648	+43·4
South-east Liège Island	64°04·0′	61°57·0′	—	0	·2285	·2662	+37·7
Cobalescou Island	64°10·5′	61°39·0′	—	0	·2362	·2975	+61·3
Diamonen Island	64°03·0′	61°16·0′	—	0	·2273	·2871	+59·8
Cape 3 miles north-east of Sterneck Island	64°09·2′	60°57·3′	—	0	·2347	·2682	+33·5
Seaplane Point	64°03·8′	60°45·6′	—	0	·2281	·2667	+38·6
Spring Point	64°18·1′	61°06·6′	—	0	·2452	·2815	+36·3
Murray Harbour	64°21·0′	61°35·0′	—	0	·2486	·3067	+58·1
Reclus Peninsula	64°30·0′	61°45·7′	—	0	·2592	·2815	+22·3
Nansen Island	64°33·2′	62°00·0′	—	0	·2629	·2974	+34·5
Bell Island	64°16·4′	61°59·2′	—	0	·2432	·2941	+50·9
Davis Island	64°06·2′	62°05·0′	—	0	·2312	·2750	+43·8
Metchnikoff Point	64°02·8′	62°34·4′	—	0	·2270	·2875	+60·5
Astrolabe Needle	64°08·8′	62°35·6′	—	0	·2342	·2754	+41·2
Buls Island	64°25·0′	62°17·0′	—	0	·2533	·2978	+44·5
Pabellón Island	64°19·1′	62°57·1′	—	0	·2464	·2958	+49·4
Eta Island	64°18·5′	62°57·2′	—	0	·2457	·2952	+49·5
Gamma Island	64°19·7′	62°59·2′	—	0	·2470	·2962	+49·2
Gand Island	64°25·5′	62°52·0′	—	0	·2539	·2901	+36·2
Cape Bayle	64°16·7′	63°11·0′	—	0	·2436	·2927	+49·1
The Hump	64°20·9′	63°11·0′	—	0	·2484	·2819	+33·5

TABLE III (*continued*)

Locality	*Latitude* (S.)	*Longitude* (W.)	*Height* (m.)	*Height Correction* (mgal)	*Theoretical Gravity at This Latitude* (cm. sec.$^{-2}$)	*Absolute Value of Gravity* (cm. sec.$^{-2}$)	*Bouguer Anomaly* (mgal)
GRAHAM LAND AND ISLANDS (*cont.*)							
False Island	64°31·2′	62°53·1′	—	0	·2606	·2967	+36·1
The Waifs	64°33·5′	62°44·0′	—	0	·2633	·3006	+37·3
Dobrowolski Island	64°36·2′	62°55·1′	—	0	·2665	·3051	+38·6
Lion Island	64°41·5′	63°09·0′	—	0	·2726	·3040	+31·4
Green Reef	64°43·5′	63°16·7′	—	0	·2749	·3057	+30·8
Canty Point	64°45·6′	63°30·6′	—	0	·2774	·3038	+26·4
Cape Lancaster	64°51·3′	63°43·0′	—	0	·2841	·3180	+33·9
Arthur Harbour	64°45·8′	64°04·7′	—	0	·2776	·3119	+34·3
Heed Rock	64°58·6′	63°47·0′	—	0	·2924	·3303	+37·9
South Bay (Doumer Island)	64°52·4′	63°34·2′	4	+0·7	·2852	·3186	+33·4
*Port Lockroy	64°49·5′	63°30·5′	—	0	982·2820	982·3067	+24·7
Lockley Point	64°47·0′	63°24·2′	—	0	·2790	·3055	+26·5
Breakwater Island	64°47·7′	63°13·5′	—	0	·2798	·3101	+30·3
Fridtjof Island	64°53·1′	63°20·0′	—	0	·2861	·3180	+31·9
Cape Errera	64°54·4′	63°36·6′	—	0	·2877	·3220	+34·3
Ménier Island	64°58·0′	63°36·5′	—	0	·2918	·3327	+40·9
Capstan Rocks	64°57·3′	63°25·6′	—	0	·2910	·3242	+33·2
Cape Willems	64°56·9′	63°14·8′	—	0	·2905	·3162	+25·7
Bruce Island	64°53·3′	63°08·0′	—	0	·2864	·3155	+29·1
Island 2 miles west of Lemaire Island	64°48·7′	63°05·8′	—	0	·2811	·3143	+33·2
South Paradise Harbour	64°54·4′	62°56·2′	—	0	·2877	·3044	+16·7
*Waterboat Point, site of Chilean pendulum station	64°49·2′	62°51·6′	4	+0·8	982·2816	982·3075	+26·7
Useful Island	64°42·5′	62°53·5′	—	0	·2738	·3044	+30·6
Rongé Island	64°44·6′	62°39·5′	—	0	·2762	·2937	+17·5
Beneden Head	64°46·0′	64°42·0′	—	0	·2779	·2952	+17·3
Neko Harbour	64°51·0′	62°32·2′	—	0	·2837	·2939	+10·2
Danco Island	64°43·5′	62°36·2′	—	0	·2749	·3037	+28·8
Spigot Peak	64°37·8′	62°34·0′	—	0	·2682	·2989	+30·7
Cape Anna	64°35·2′	62°26·0′	—	0	·2650	·2987	+33·7
Emma Island	64°36·8′	62°18·5′	—	0	·2670	·2912	+24·2
Pelseneer Island	64°40·7′	62°11·7′	—	0	·2716	·2820	+10·4
Moureaux Islands	65°05·0′	63°07·0′	—	0	·2999	·2973	−2·6
Lemaire Channel (1)	65°03·0′	63°53·0′	—	0	·2976	·3259	+28·3
Lemaire Channel (2)	65°09·0′	64°05·0′	—	0	·3045	·3218	+17·3
Petermann Island	65°10·4′	64°08·3′	—	0	·3060	·3361	+30·1
Moot Point	65°12·3′	64°04·6′	3	+0·6	·3083	·3462	+37·9
Cape Tuxen	65°16·2′	64°07·6′	—	0	·3128	·3512	+38·4
*Galindez Island	65°14·6′	64°16·0′	9	+1·7	982·3109	982·3423	+33·1
Irizar Island	65°13·1′	64°12·0′	—	0	·3092	·3397	+30·5
Uruguay Island	65°14·0′	64°13·3′	—	0	·3102	·3421	+31·9
Winter Island	65°14·9′	64°15·5′	—	0	·3113	·3433	+32·0
Three Little Pigs	65°14·4′	64°16·8′	—	0	·3107	·3435	+32·8
The Barchans	65°14·4′	64°18·0′	—	0	·3107	·3421	+31·4
Anagram Islands (1)	65°12·4′	64°21·0′	—	0	·3084	·3523	+43·9
Anagram Islands (2)	65°12·1′	64°19·0′	—	0	·3080	·3521	+44·1
Somerville Island	65°23·0′	64°18·0′	26	+5·1	·3205	·3491	+33·7
Woolpack Island	65°37·5′	64°59·0′	—	0	·3370	·3697	+32·7
Marie Island	66°08·2′	65°48·5′	—	0	·3716	·4013	+29·7
Cape Leblond	66°02·7′	66°36·0′	—	0	·3655	·4068	+41·3
Mist Rocks	66°48·2′	66°38·0′	—	0	·4158	·4509	+35·1
Orford Cliff	66°55·0′	66°30·0′	—	0	·4232	·4314	+8·2
*Detaille Island	66°52·5′	66°49·0′	5	+1·0	982·4205	982·4530	+33·5
Sillard Islands	66°39·4′	67°34·0′	—	0	·4061	·4427	+36·6
*Southern Adelaide Island	67°46·0′	68°55·0′	4	+0·8	982·4779	982·5221	+45·0
Cape Alexandra	67°45·4′	68°37·0′	—	0	·4773	·5168	+39·5
Dion Islands	67°51·6′	68°41·0′	—	0	·4838	·5290	+45·2
*Stonington Island	68°11·3′	67°00·5′	17	+3·3	982·5045	982·5125	+11·3
*Fossil Bluff	71°20·0′	68°17·0′	39	+7·7	982·6893	982·6672	−14·4

Heights of stations have been omitted if they are estimated to be less than 3 m.
No height correction has been made for stations within 3 m. of sea-level.

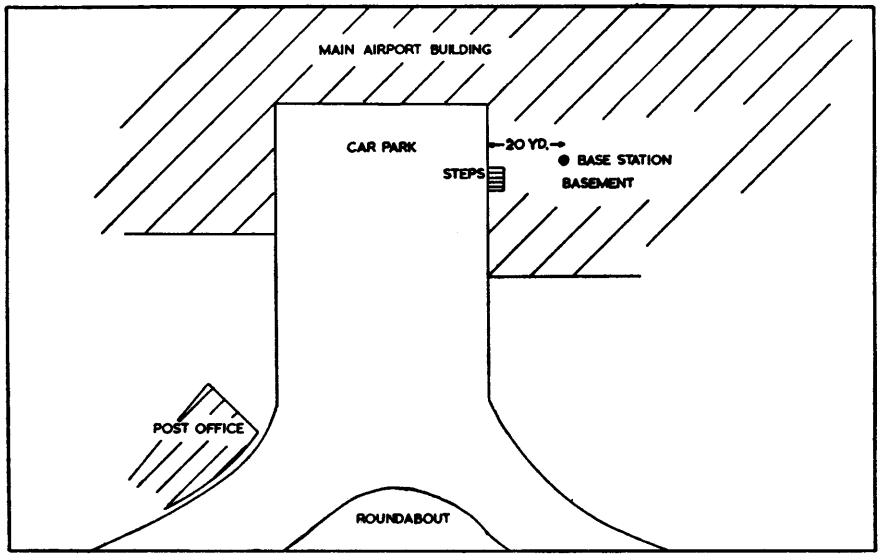

FIGURE 3

Gravity base station: Buenos Aires, Argentina. Professor Baglietto's station in the basement of the airport terminal at the International (Ezeiza) Airport. The station is about 20 ft. (6·1 m.) in from the access steps.

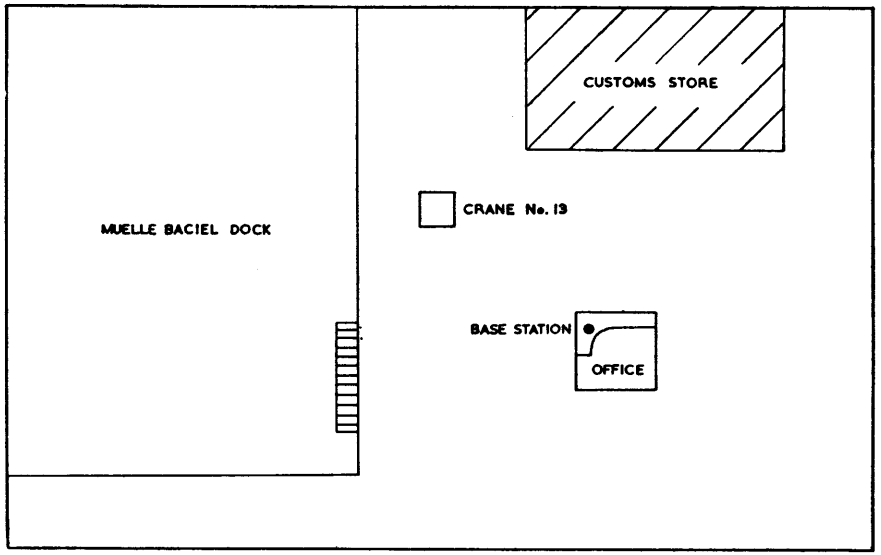

FIGURE 4

Gravity base station: Montevideo, Uruguay. The station is on the tiled surround to the pilot's office alongside No. 13 crane on the quayside of Muelle Baciel.

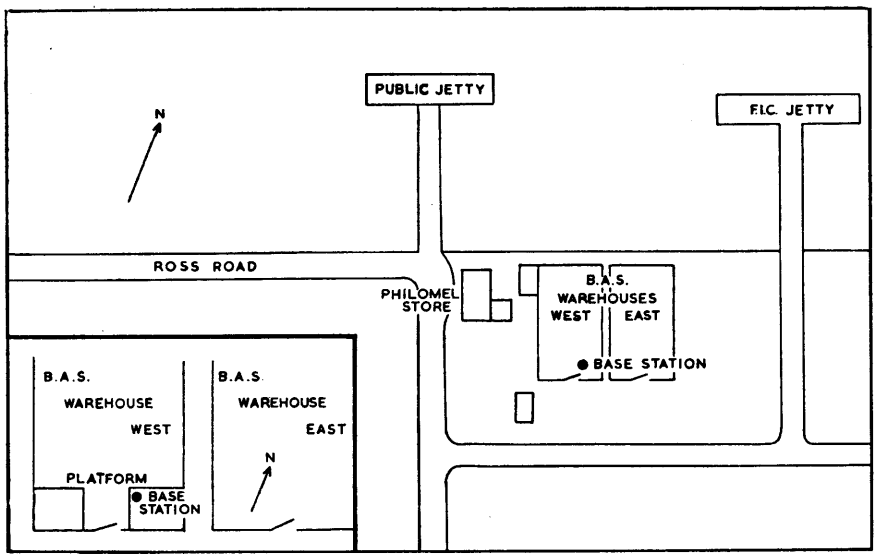

FIGURE 5

Gravity base station: Port Stanley, Falkland Islands. The station is on the corner of a concrete loading platform inside the westernmost British Antarctic Survey warehouse near the public jetty. It is marked by a chiselled cross.

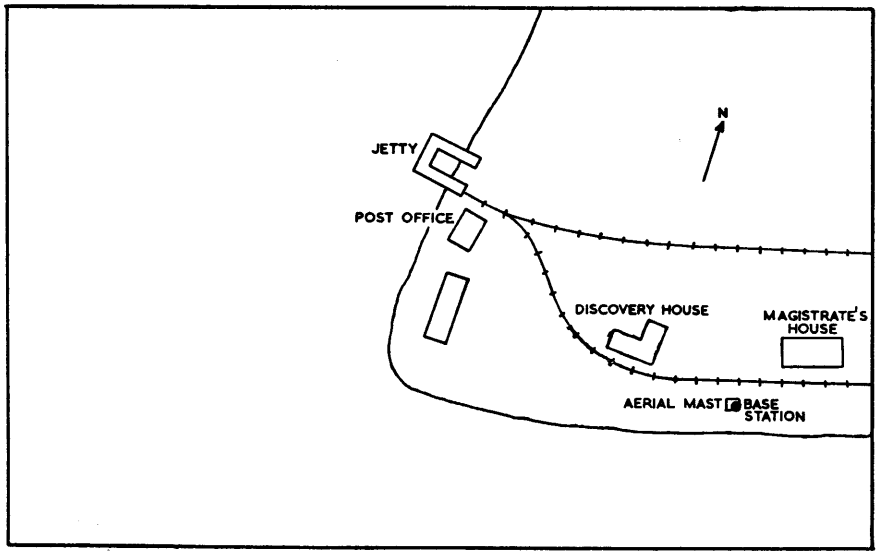

FIGURE 6

Gravity base station: King Edward Point, South Georgia. The station is on the concrete base of the wireless mast between the railway line and the beach on the south side of King Edward Point. It is marked by a brass plate.

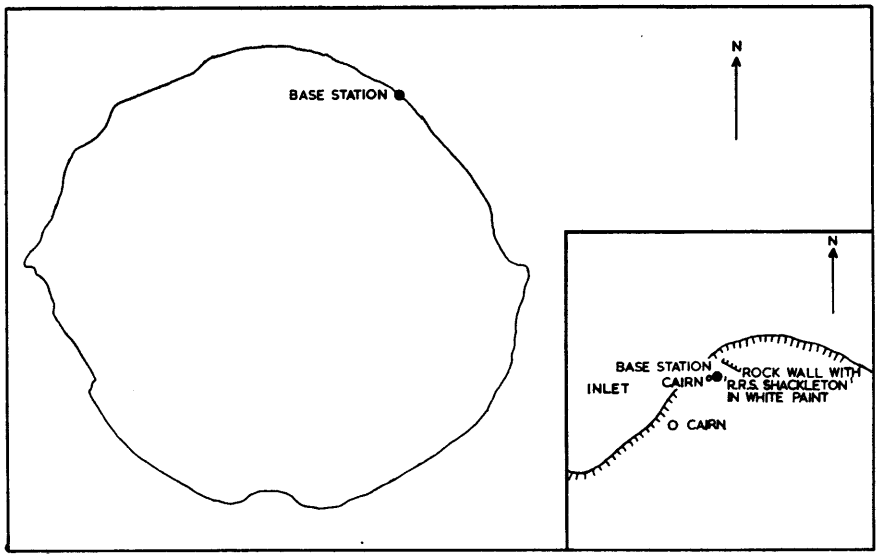

FIGURE 7

Gravity base station: Zavodovski Island, South Sandwich Islands. The station is on the cliffs of columnar lava on the north-east coast of the island. The locality is marked by a large survey cairn 6 ft. (1·8 m.) high to the south-west of the base station. The base station itself is identified by a smaller cairn 2 ft. (0·6 m.) high.

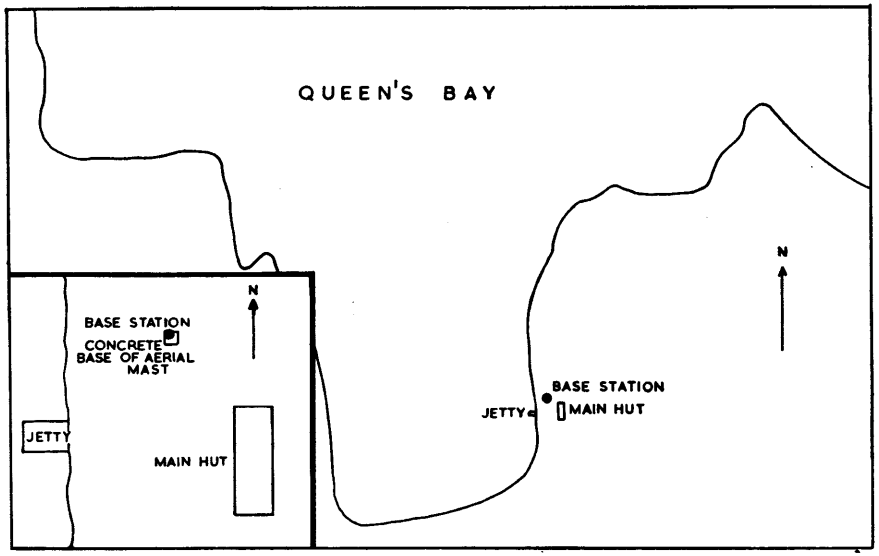

FIGURE 8

Gravity base station: Signy Island, South Orkney Islands. The new station is on the winch block in front of the hut. It is marked by a brass plate.

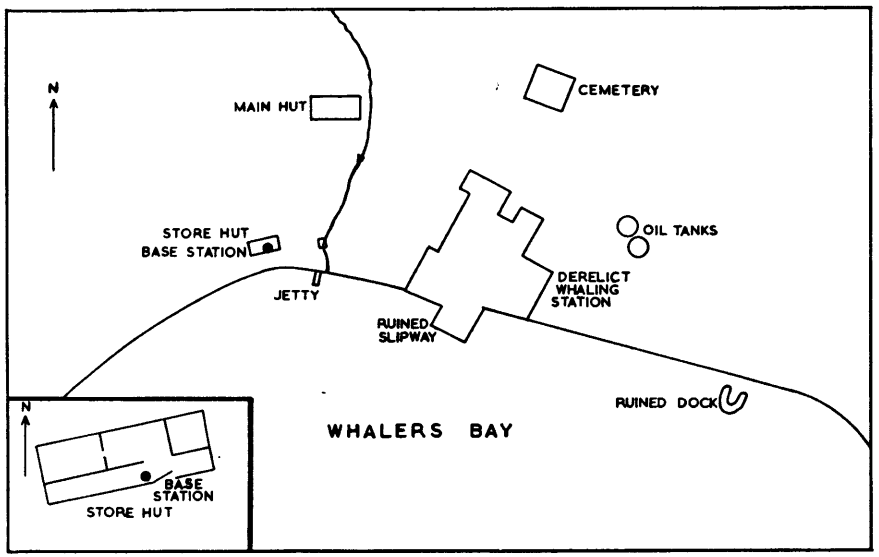

FIGURE 9

Gravity base station: Deception Island, South Shetland Islands. The station is on the concrete floor, 2 ft. (0·6 m.) down from the door, inside the old boat shed, which is now used as a store. It is marked by a brass plate.

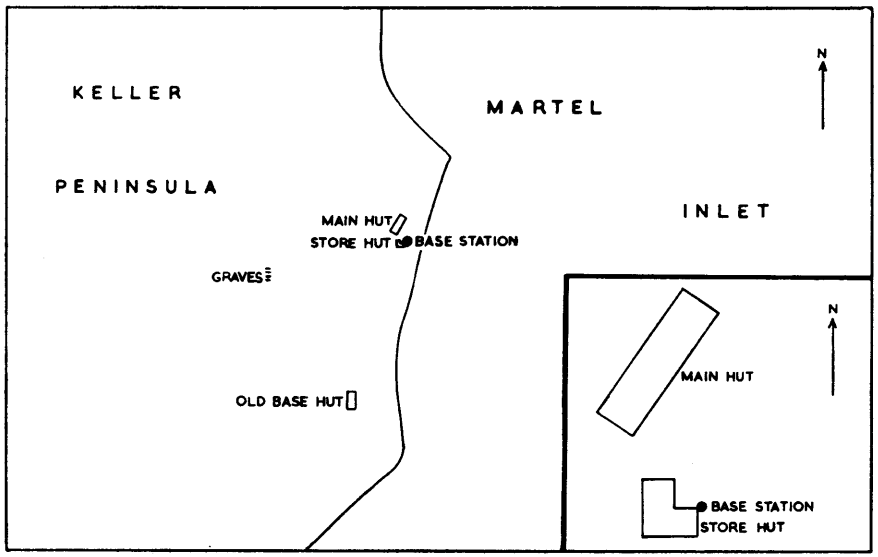

FIGURE 10

Gravity base station: Admiralty Bay, King George Island, South Shetland Islands. The station is on a concrete platform outside the black painted stores hut on the seaward side of the main hut. It is marked by a brass plate.

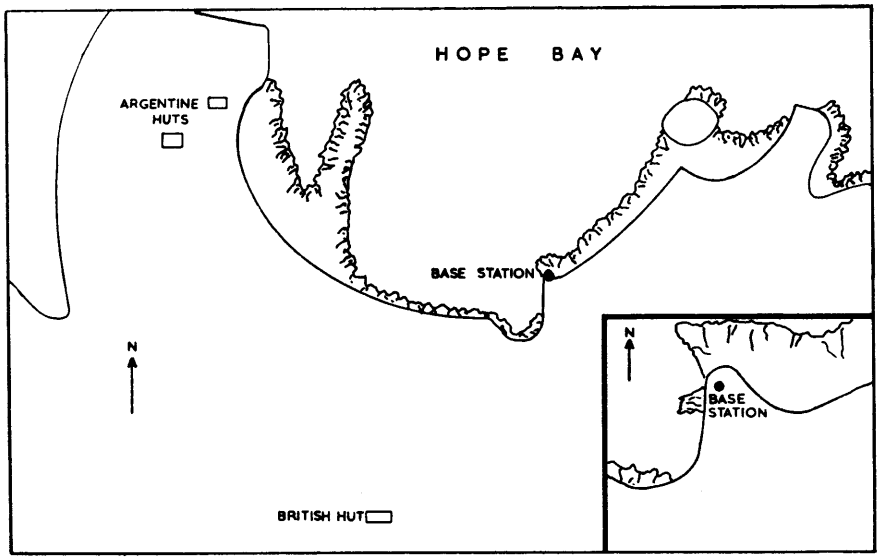

FIGURE 11

Gravity base station: Hope Bay, Trinity Peninsula. The station is on a flat concrete slab on rocks immediately above the remains of the jetty. It is marked by a brass plate.

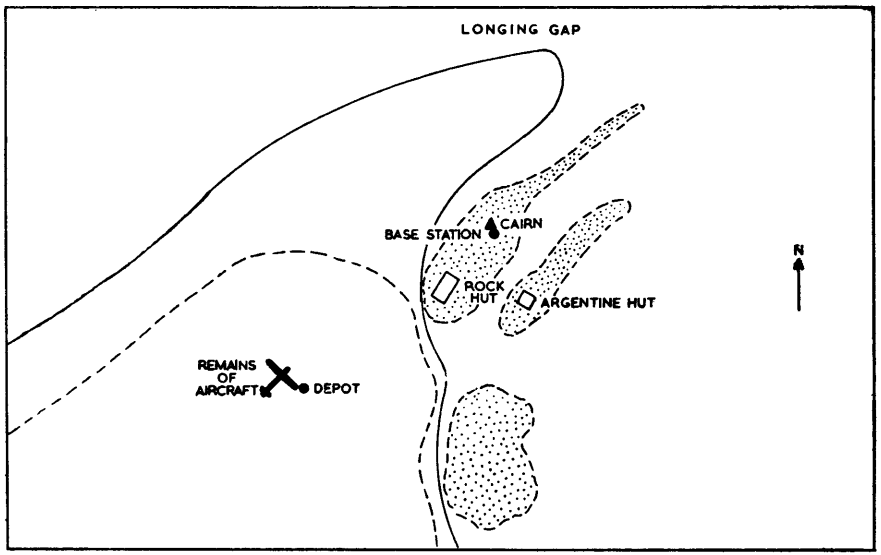

FIGURE 12

Gravity base station: north of Cape Longing, Trinity Peninsula. The station is at the foot of the astrofix survey cairn on a spur of land, at Longing Gap, 8 miles (12·9 km.) north of Cape Longing.

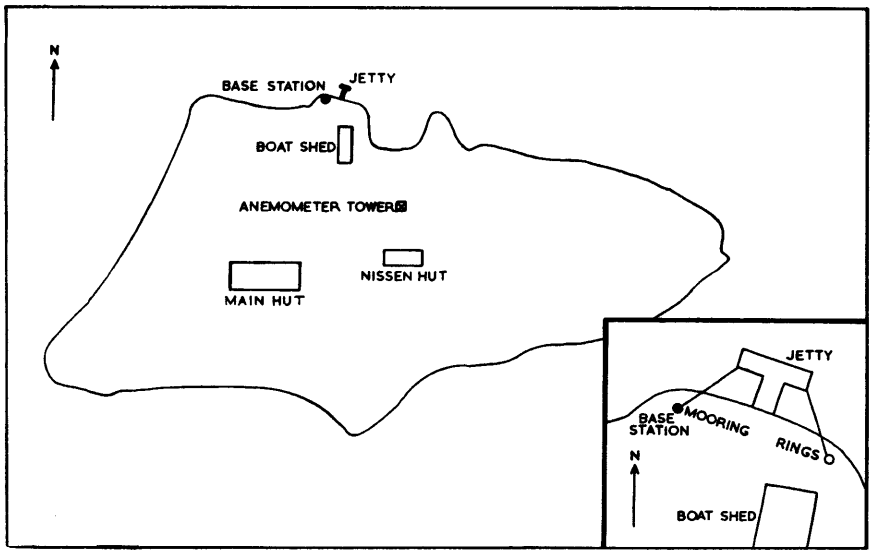

FIGURE 13

Gravity base station: Port Lockroy, Danco Coast. The station is over a mooring ring on a flat rock on the south-west side of the jetty on Goudier Island. It is marked by a brass plate.

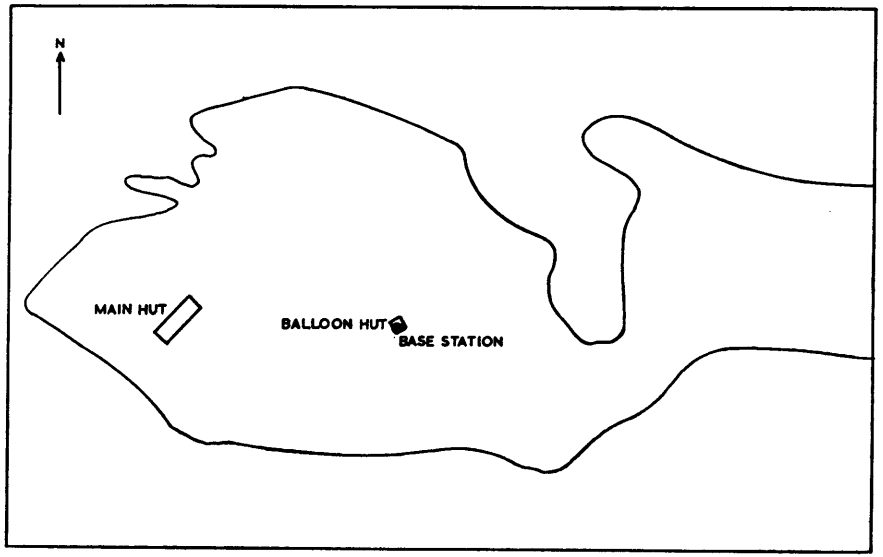

FIGURE 14

Gravity base station: Galindez Island, Argentine Islands. The station is on the flat concrete floor of the balloon hut at the British scientific station. It is marked by a brass plate.

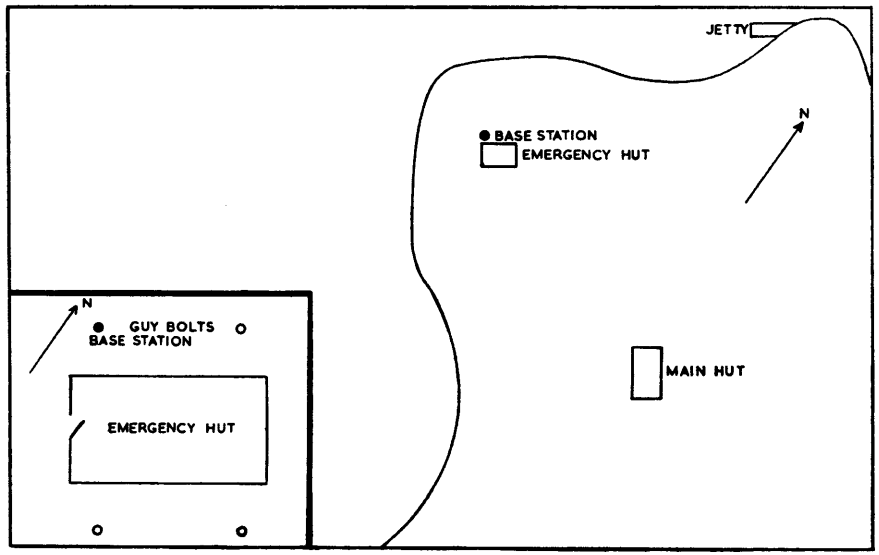

FIGURE 15

Gravity base station: Detaille Island, Loubet Coast. The station is over a guy bolt on a concrete block on the seaward side of the emergency store hut at the British scientific station.

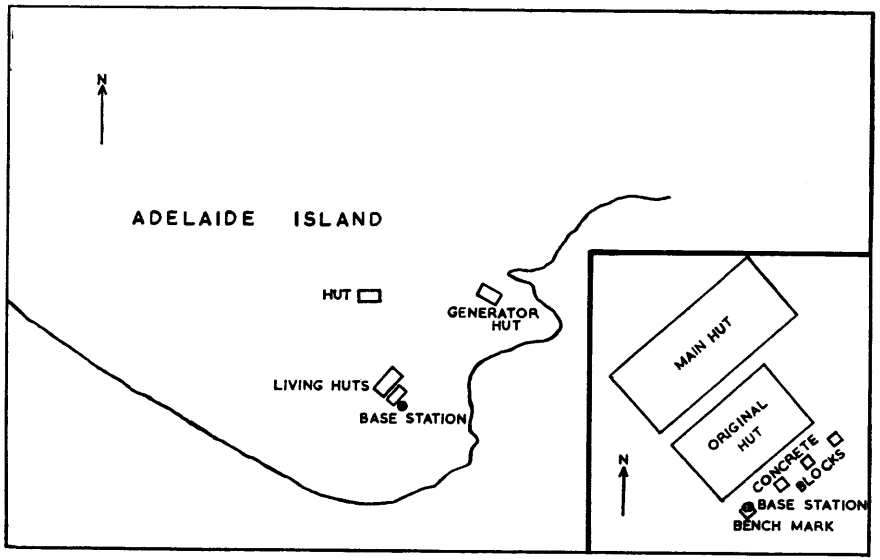

FIGURE 16

Gravity base station: southern Adelaide Island. The station is on the bench mark on a concrete block on the south side of the old living hut. It is marked by a brass plate.

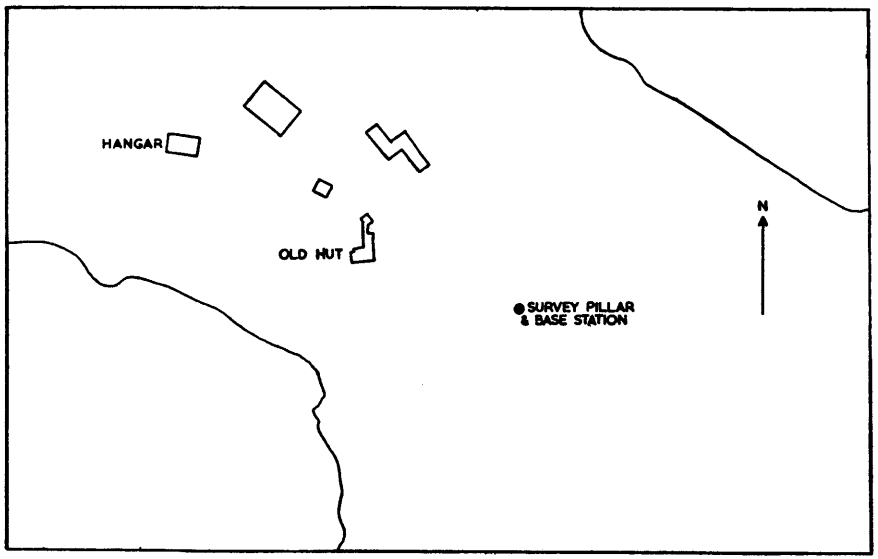

FIGURE 17

Gravity base station: Stonington Island, Marguerite Bay. The station is on top of the survey pillar between the old and new huts.

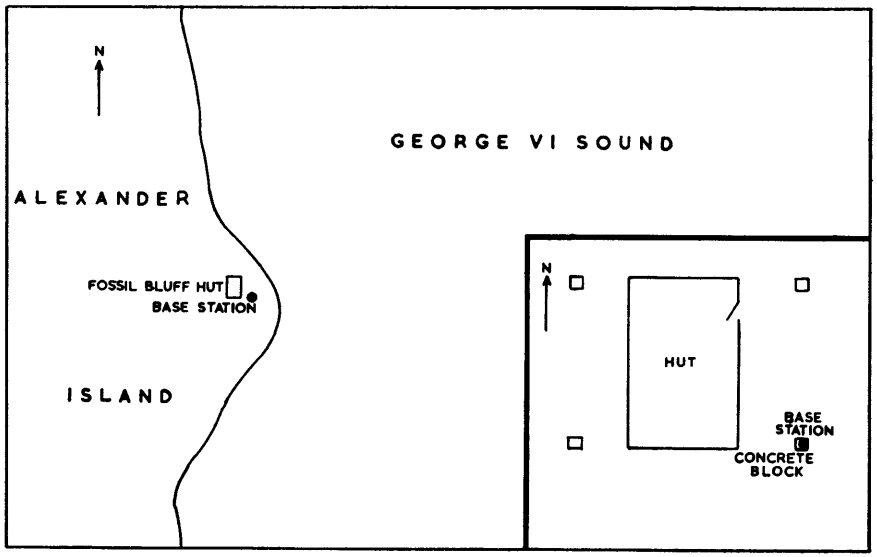

FIGURE 18

Gravity base station: Fossil Bluff, Alexander Island. The station is on a concrete guying block on the south-east side of the hut. It is marked by a brass plate.

International Gravity Formula. In making these corrections it is therefore necessary to know the station positions as accurately as possible. These were taken from the relevant Admiralty charts, mainly on a scale of 1 : 500,000. More accurate positions for some stations were obtained by using charts on a scale of 1 : 50,000 but these are only available for limited areas. Unfortunately not all the Antarctic charts are completely reliable, and there are probably errors of as much as a mile or more in the positions of some stations. The corresponding error in the Bouguer anomaly in these latitudes is about 1 mgal.

In correcting observations to sea-level it is necessary to allow for both the effect of the free-air gradient of gravity and for the attraction of the mass of rock between the station and sea-level. Since heights above sea-level were small it was possible, without introducing significant errors, to assume for the purpose of these calculations a constant density of 2·7 g./cm.^{3} for all the rocks.

The Bouguer anomaly is defined as *observed gravity+elevation correction+topographic correction—theoretical gravity at sea-level.* If we are interested only in local geological structure it is the relative values of the anomalies that are important. In the Dependencies the relative values of the observed gravity values are likely to be correct to a few tenths of a milligal. Errors in elevation correction will be equally small, but the topographic corrections, which have not so far been made, may often be a few milligals. Far less frequently, errors in the value taken for theoretical gravity, due to incorrect position finding, may also reach milligals. Thus the relative values of the Bouguer anomalies are likely to be much less accurate than those of observed gravity. Even so the regional trend of the contours (Fig. 19) based on these values must be substantially correct. Their absolute value depends on the accuracy of the gravity link with Buenos Aires which has already been discussed.

Bouguer anomalies at stations in South Georgia, the South Sandwich Islands, the South Orkney Islands and the Elephant and Clarence Islands are shown in Figs. 20, 21, 22 and 23. Wherever possible, stations were observed within about 3 ft. (0·9 m.) vertically of the sea. Since the tidal range is no more than 6 ft. (1·8 m.), these stations were therefore within about 6 ft. (1·8 m.) of mean sea-level. No elevation correction has been applied to these stations but the resulting maximum error cannot be more than 0·5 mgal. The heights of stations which could not be observed near sea-level were determined using a staff and level wherever this was possible. The heights of a few awkwardly placed stations were estimated.

In hilly and mountainous country, or on the edge of deep water, the effect of topography at a station is likely to be important. Where good maps and charts are available this effect can be calculated graphically and an allowance made for it. Available maps and charts of this region are not sufficiently detailed to permit more than rough calculations of its magnitude to be made, and so far this has only been done for a few typical stations. It appears that at most of the stations measured the effect will not be greater than about 3 mgal, though at a few it will exceed this, reaching perhaps 5 or 6 mgal. At one or two stations it is likely to be even greater.

5. *Interpretation*

Until the seismic refraction lines shot in Bransfield Strait have been fully interpreted only a general and tentative assessment of the gravity data can be given. As shown in Fig. 19, the gravity contours follow the structural trend of the arc, and are everywhere positive. The main feature is the gradual increase in value towards the north-west. A station near Cape Longing on the east coast of Graham Land has a Bouguer anomaly of +55·2 mgal, which suggests that there may be a minimum over the centre of the peninsula. No data are available for Bransfield Strait but in this area measurements at Deception Island, where the Bouguer anomaly is about +50 mgal, suggest that the anomaly reaches a maximum over the strait, and drops again at Deception Island. It then rises to +130 mgal in a sharp elongated high centred over the South Shetland Islands.

The average gradient over Bransfield Strait is about 1·5 mgal/nautical mile (0·8 mgal/km.). This gradient is so general a feature that it is likely to be due to lateral changes in the thickness of the crustal layers. If the Mohorovičic discontinuity is accepted as the main density contrast, then using the density values of 2·84 and 3·27 g./cm.^{3} for the crust and mantle, as given by Worzel and Shurbet (1955), the variation in crustal thickness can be determined. This was done graphically and is shown in Fig. 24. The depth to the interface was calculated at a point at the eastern end of the profile where the rate of change in thickness is a minimum. Accepting Worzel and Shurbet's value of 33 km. for crustal thickness in low-lying continental areas where the Bouguer anomaly is small, then at the eastern end of the section where the anomaly is 90 mgal the thickness will be 28 km., provided the area is in isostatic equilibrium.

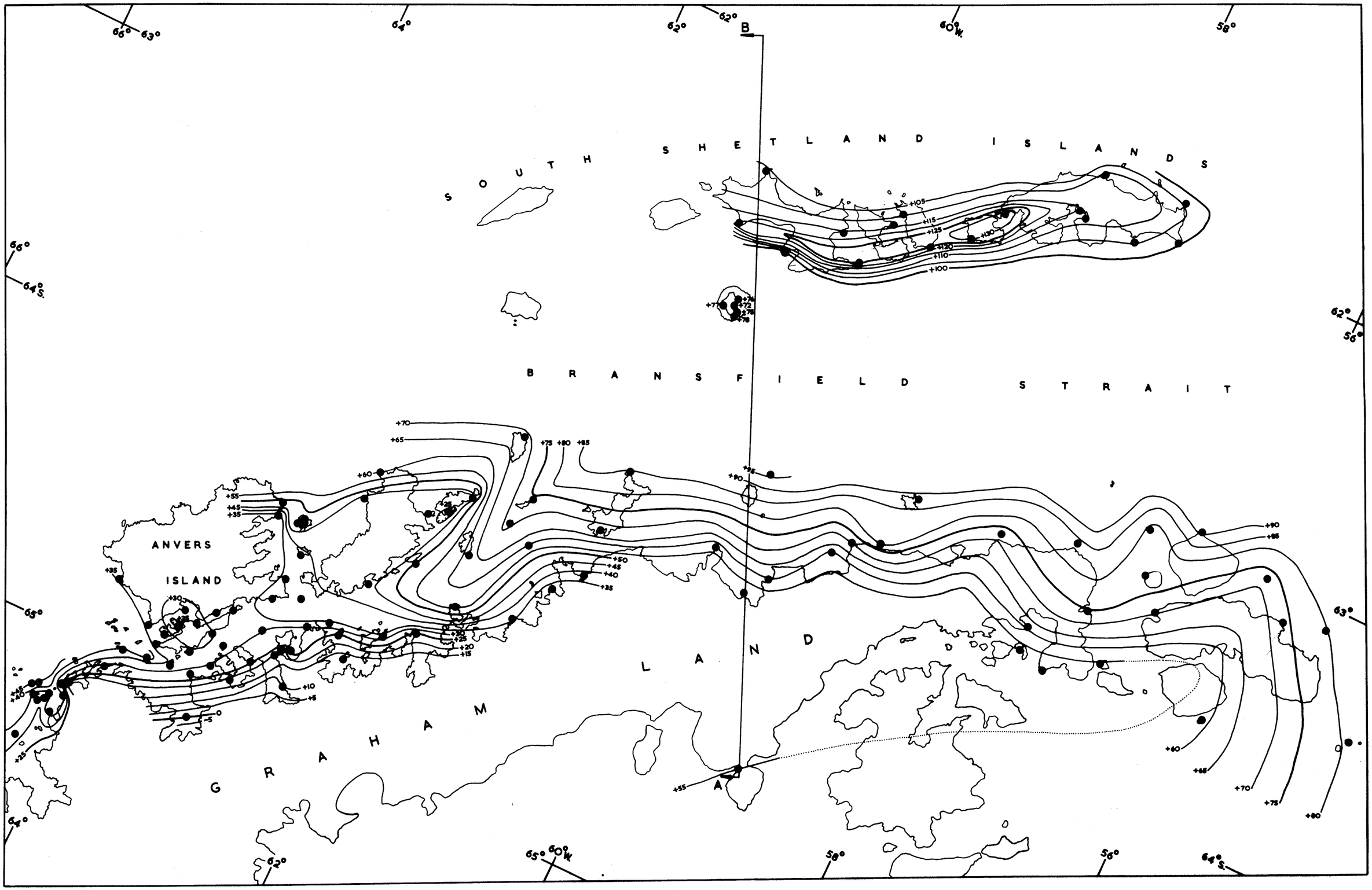

FIGURE 19

Bouguer anomalies in the Bransfield Strait area. The contour interval is 5 mgal. AB is the line of section in Fig. 24.

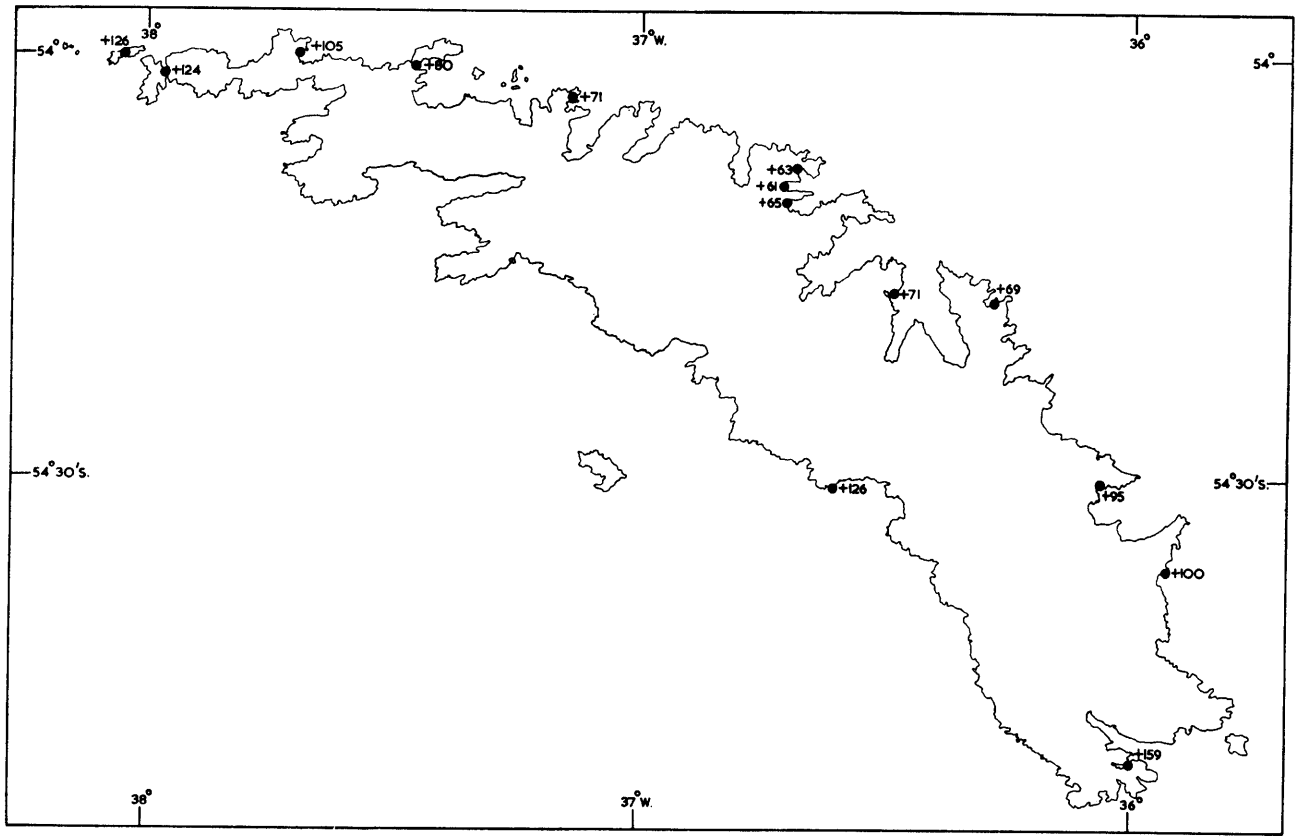

FIGURE 20
Bouguer anomalies (in mgal); South Georgia.

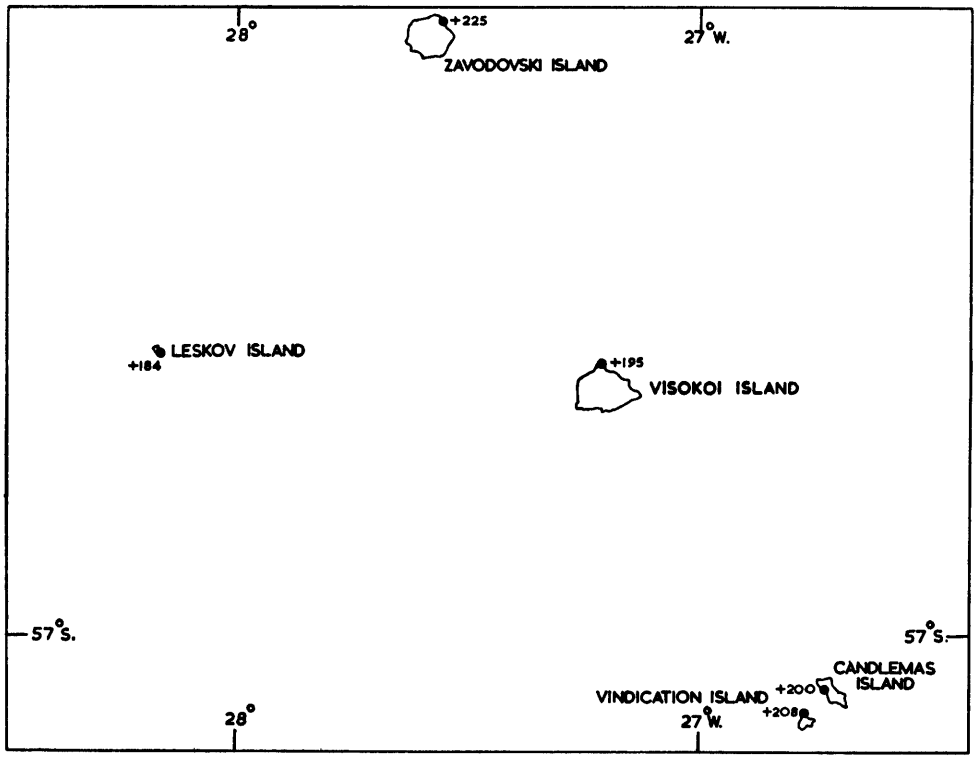

FIGURE 21
Bouguer anomalies (in mgal); South Sandwich Islands.

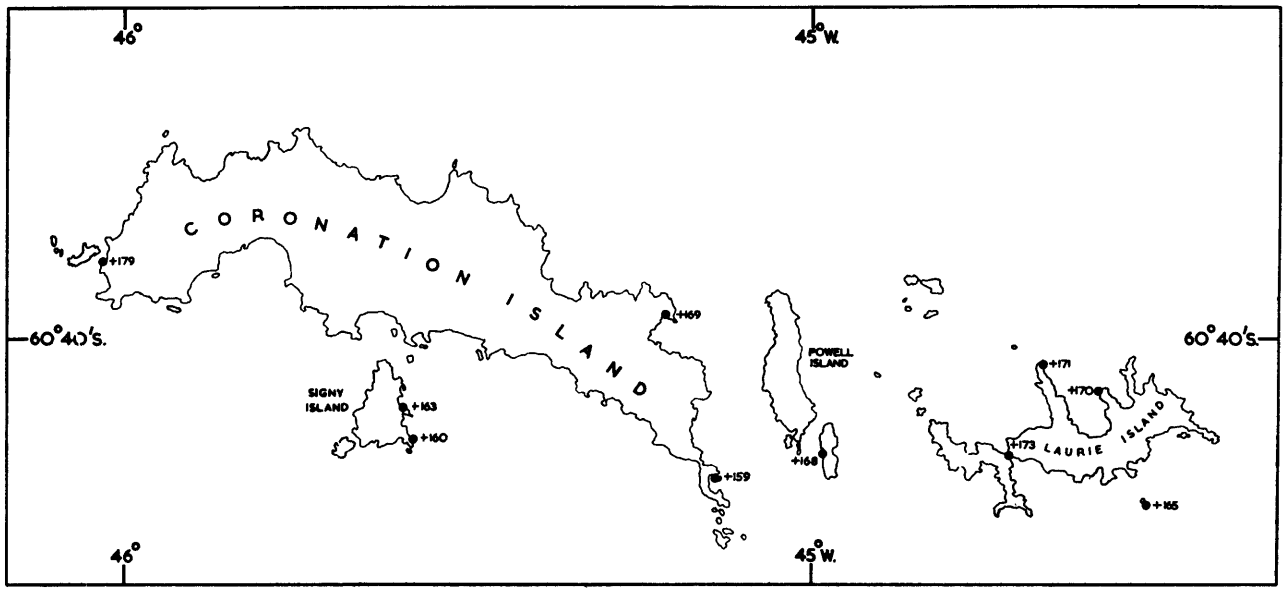

FIGURE 22
Bouguer anomalies (in mgal); South Orkney Islands.

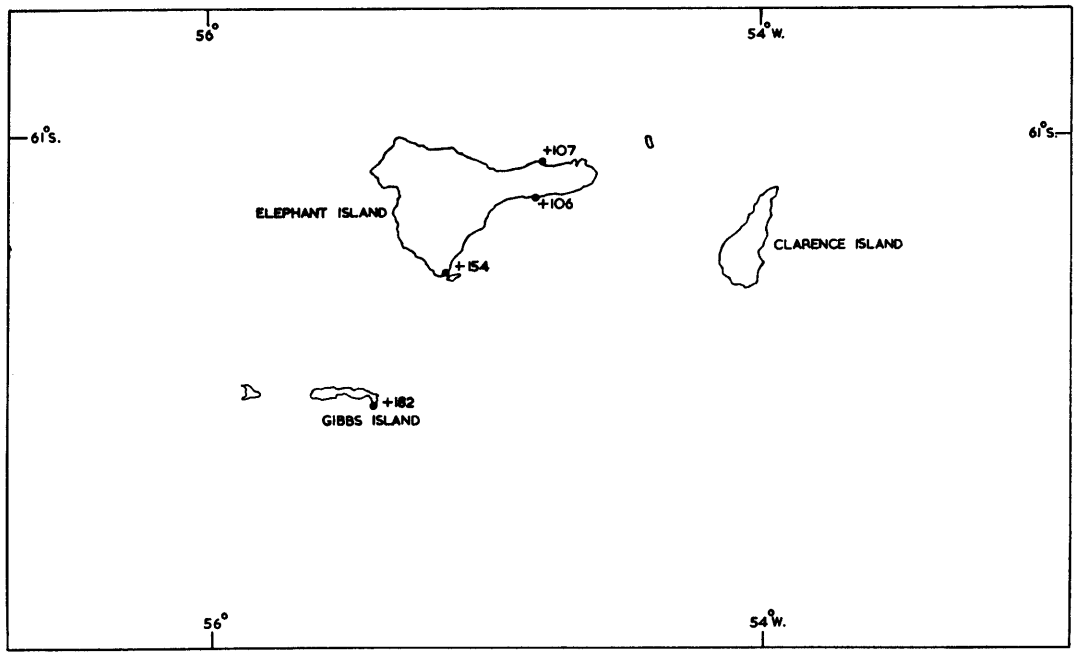

FIGURE 23
Bouguer anomalies (in mgal); Elephant and Clarence Islands group.

A new analysis by Woollard and Strange (1962) which uses considerably more data shows that the density contrast between the crust and the mantle is not constant and varies with crustal thickness, but the empirical relationship which they give cannot be applied in this area for the reason already mentioned, i.e. that the thickness variations appear to be relatively rapid, whereas in the areas to which the data apply this is not so. There is, of course, a further and even more important source of error in all calculations of this kind. The scatter of individual points from the empirically derived curves relating seismic depths and Bouguer anomalies indicates that depths derived from gravity measurements alone are subject to considerable uncertainties. The cross-section given in Fig. 24 must therefore be taken as illustrating qualitatively rather than quantitatively the changes in crustal thickness along the line of section.

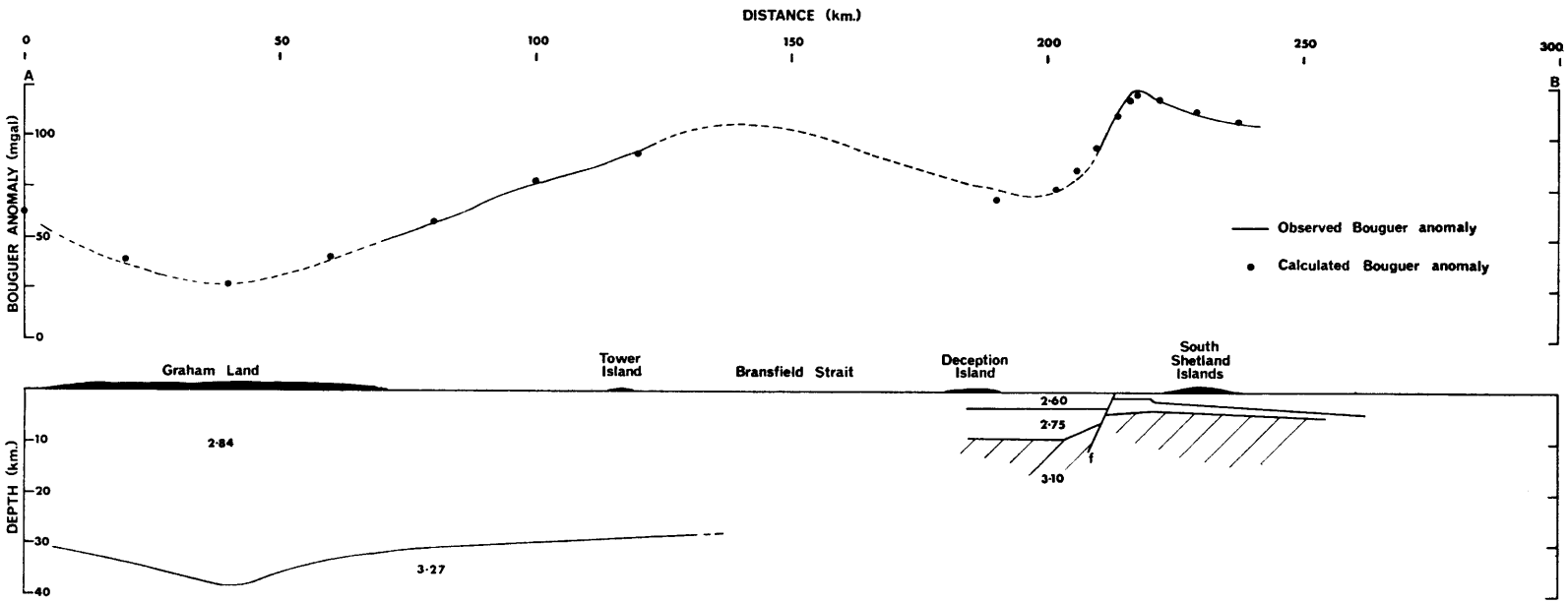

FIGURE 24

Gravity profile and interpretation along the line AB in Fig. 19. The densities given are based on the known seismic velocities.

The gradient on the south-east flank of the narrow ridge of high gravity over the South Shetland Islands is too steep for the high to be attributed entirely to a change in the thickness of the crust. It must be due mainly to a density change at a much shallower depth.

A provisional interpretation of seismic refraction lines in Bransfield Strait indicates the presence of a layer with a velocity of 7·4 km./sec. at about 8 km. depth, overlain by two layers with velocities of 5·8 km./sec. and 3·1–3·7 km./sec. The gravity high is attributed to uplift of the higher-velocity and presumably higher-density layers which are of the size and form also shown in Fig. 24.

Density contrasts at greater depths, such as at the Mohorovičic discontinuity, would result in a much wider anomaly than that observed; although some elements of the structure may be of shallower depth than calculated, it is probable that the general form shown is correct.

III. THE MAGNETIC SURVEY

A. Instrumentation and Survey Procedure

All the magnetic measurements have been made with a proton magnetometer. The detecting head of the instrument, which is in a watertight container, is towed behind the ship at a distance sufficiently great for the strength of the field due to the ship's magnetization to be negligible. The recording apparatus is installed at a convenient position within the ship. Such an instrument measures the absolute value of the total magnetic field, and an accuracy of 1 gamma (10^{-5} oersted) can be achieved.

During the 1959–60 and 1960–61 seasons the instrument used was one designed and built by Dr. F. Gray and loaned by the Department of Geophysics, Imperial College of Science. In many respects it proved to be satisfactory, but much difficulty was experienced during the first season, mainly due to leaks in the towed units. The precession signal received at the ship was also difficult to measure at times because of electrical interference. These troubles were overcome in the second season by redesigning the towed unit and replacing the valve pre-amplifier by a transistorized version which provided a stronger signal. The ship's a.c. generator was also suppressed.

The instrument was arranged to measure and record every 30 sec., and from the record, determinations of field strength could be made with an accuracy of ± 10 gamma. For our purposes this was considered sufficient, since no satisfactory correction to the data for the daily variation in the strength of the Earth's magnetic field could be made.

During the 1961–62 season a magnetometer made by Messrs Bruce Peebles Ltd. of Edinburgh was used. This instrument is the property of the Department of Scientific and Industrial Research, but was loaned by the Department of Geodesy and Geophysics, University of Cambridge, who have custody of it. It records the field strength every 30 sec. with an accuracy of ± 1 gamma. The instrument worked very satisfactorily and only a few minor faults have occurred.

Continuous soundings were taken throughout the survey. All navigation was done by the ship's officers, positions being fixed from morning and evening star sights and noon sights when the weather permitted. The estimated accuracy of the positions is ± 2 miles* ($\pm 3·7$ km.). Within range of land positions were fixed frequently using radar bearings and ranges, the estimated accuracy of which is about $\pm 0·5$ miles (0·9 km.).

Although it was not possible to make any diurnal correction to the magnetometer records, observatory data from the Argentine Islands station have been used to check on the occurrence of magnetic storms and very disturbed days. No major storms occurred during the course of the survey and it is therefore probable that corrections for short-period variations would not amount to more than 50 gamma except on particularly disturbed days. This figure is of the same order as many of the smaller anomalies but, as these are traversed in a time short compared with the period of the daily variation, this has a relatively small effect on their amplitude and form. The absence of a diurnal check is of more importance when attempting to contour an area such as Bransfield Strait. Here, track intersections show large discrepancies which are due at least in part to this cause. The other and equally important cause is navigational error. Since the local field gradients in an area like Bransfield Strait may be as great as

* Throughout this report the "mile" unit used refers to "nautical miles", i.e. 1·852 km.

several hundred gamma per mile, an error in navigation of 0·5 miles (0·9 km.) in fixing the intersection of one track with another can lead to mis-ties comparable to and even greater in magnitude than those due to diurnal change.

Because different tracks in the same area were surveyed at different times, separated by either months or years, all measurements had to be reduced to the same epoch to allow for the secular change in the magnetic field. The rate of change of the total field, obtained from the Argentine Islands observatory data for 1957–60, was constant at +126 gamma/yr. when averaged over the whole period. Two sets of measurements made about one year apart on quiet nights at Port Stanley (28 December 1961 and 7 January 1963) and South Georgia (19 December 1961 and 15 January 1963) gave about the same rate of change. A convenient figure of 120 gamma/yr. was therefore adopted for correction purposes, and all measurements were reduced to December 1961. Considering the lack of diurnal control and the errors resulting from navigational inaccuracies, the adoption of a constant value for the secular variation over the whole region was justifiable.

When carrying out a magnetic survey it is normal practice to traverse the area at a sufficiently close spacing to make possible the preparation of a contour map showing the spatial variation of the strength of the magnetic field. From the general form of this map and from the trend, magnitude and shape of the various magnetic features it is then possible to deduce information about the geological structure. Interpretation is often qualitative rather than quantitative, but structural trends and major boundaries can be mapped; in some circumstances depths to magnetic bodies may be determined. Where there is seismic information which can be used for control, interpretation is likely to be more reliable, and to some extent the magnetic data can be used to interpolate structure between seismic traverses.

It was clearly impossible to carry out a systematic survey by ship of even a significant fraction of the Scotia Sea in which the track lines would be sufficiently close to permit contouring. To choose a limited area for close study seemed more feasible, but no information existed to show which areas were likely to be interesting, and detailed surveying involved the problem of accurate navigation. Also, the amount of ship's time available for this kind of work was limited. For these reasons no detailed survey has been attempted, and the procedure has been to operate the magnetometer whenever the ship has been at sea, diverting it from its usual routes when necessary so that no track has been covered twice. Any other available time has been used to make a systematic reconnaissance of particular areas not normally visited in the course of the ship's routine duties. Fig. 25 shows all the magnetometer traverses made up to the end of the 1961–62 season. Though there are still considerable gaps, some parts of the area have now been quite well covered. With the exception of the Bransfield Strait area the tracks are 30 miles (56 km.) or more apart, which is too great a distance for contouring to be possible; except in a few places it is not even possible to correlate individual magnetic features from one track to another. It has been necessary therefore to try and develop interpretation methods for dealing with the data.

B. The Regional Gradient

In Fig. 26 contours have been drawn for the total intensity of the magnetic field at 500 gamma intervals over the area of the Scotia Sea. These are based on smoothed values of the magnetic field obtained from measurements taken along the longer tracks shown in Fig. 25. A correction of 120 gamma/yr. has been made for secular variation and the data have been reduced to December 1961. Only an approximate averaging procedure was used, since the amount and distribution of the data did not appear to justify the use of any elaborate method. At this stage the contours must therefore be considered as tentative. Over the open sea the gradient is approximately 14 gamma/nautical mile (7·6 gamma/km.) in a south-south-west direction.

C. The Scotia Sea

1. *Analysis of the magnetic features*

The data are shown in Fig. 25 and consist of a number of tracks along which the variations in strength of the Earth's total magnetic field are known. Along most of the tracks the water depth has also been measured. In some areas, for example Drake Passage and between the Falkland Islands and South Georgia, several roughly parallel traverses have been made, most of them about 50 miles (95 km.) apart.

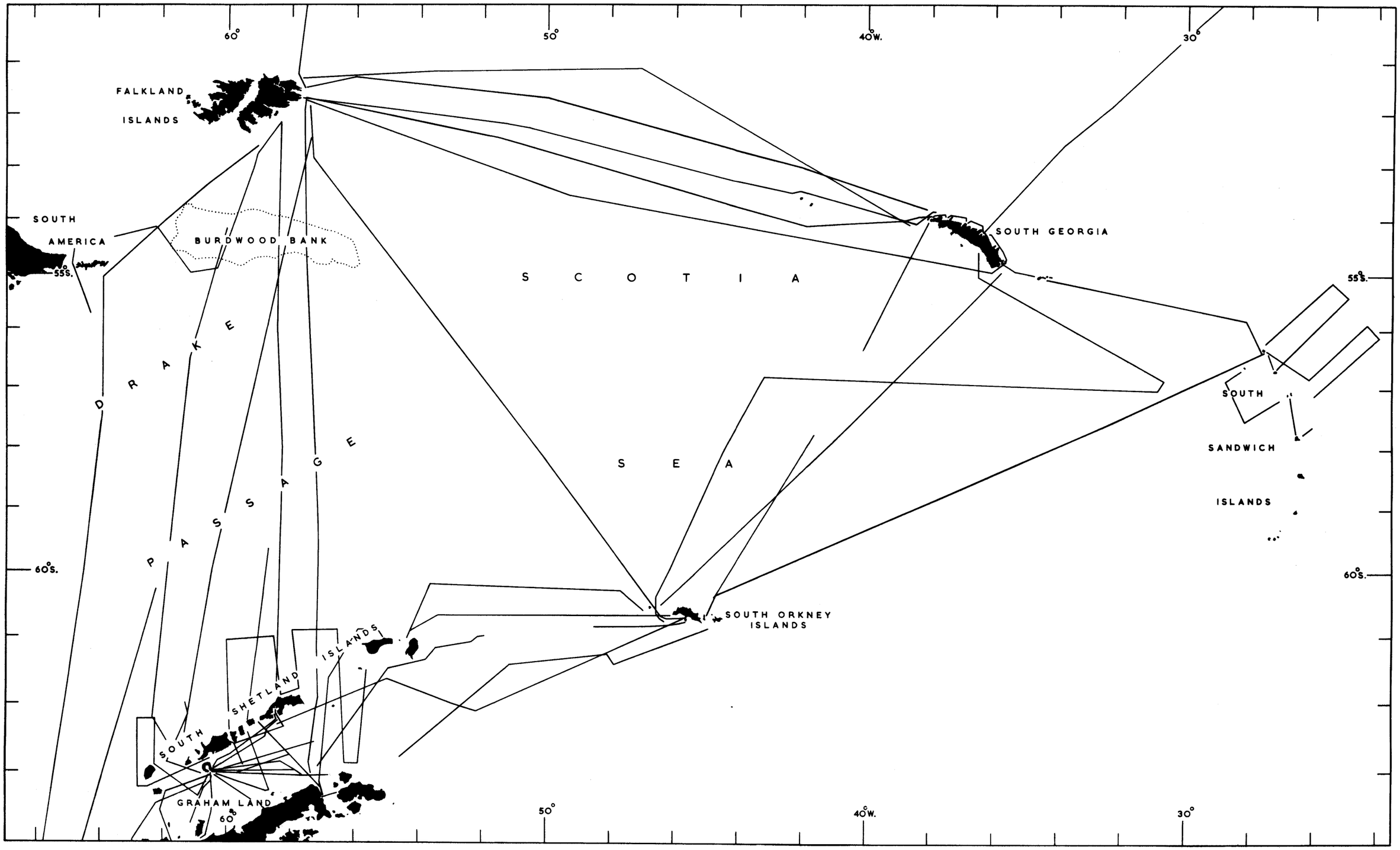

FIGURE 25

Map of the Scotia Arc showing the main magnetic traverses completed by the end of the 1961–62 season.

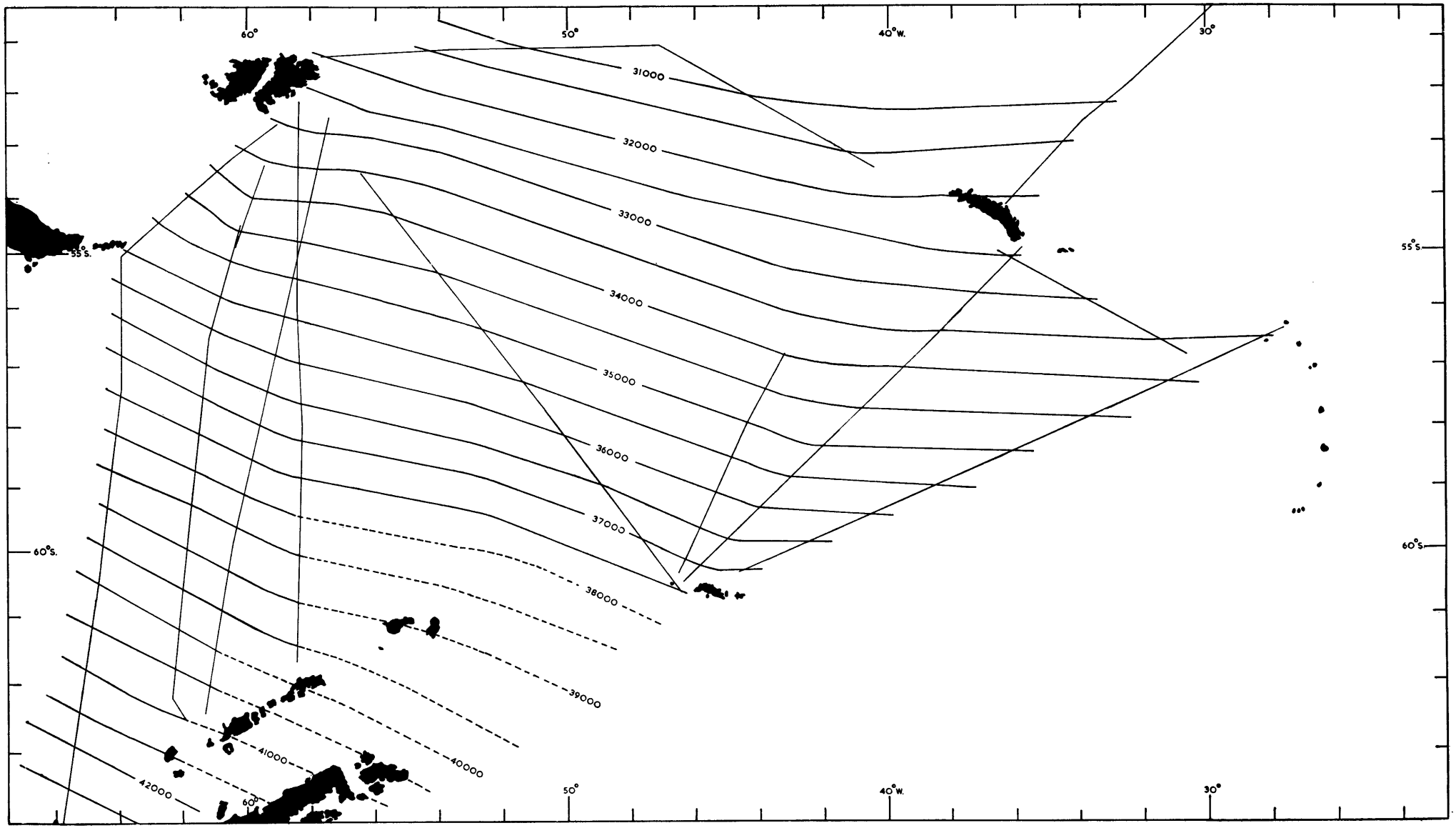

FIGURE 26

Total field regional magnetic contours in the Scotia Sea. The contour interval is 500 gamma.

In magnetic surveying the anomalies of interest are those that have a width of a few miles and are caused by lateral changes in the nature of the crustal layers. The regional magnetic gradient due to the Earth's main field has to be subtracted from the observations so that interpretation can be carried out on the resultant residual anomalies.

In this region the magnetic field has only been measured along widely spaced tracks, and hence the information available about each individual anomaly is a cross-section, the relation of which to the anomaly itself (as defined by a contour map of field strength variation) is unknown. It is obvious, therefore, that the amplitude and shape of a magnetic feature, i.e. any cross-section of an anomaly, on a track will depend considerably on how the track cuts the anomaly. Thus, when it is not possible to contour the area or recognize trend lines (as is the case in this area), only a very limited amount of information can be obtained from the study of individual features. An attempt has therefore been made to analyse all well-marked features on a statistical basis. A preliminary study was made of a large area in Drake Passage to the south of the Burdwood Bank, which seemed particularly suitable for this purpose. This area is crossed by five tracks, all running roughly parallel from north to south. There are also indications from the bathymetric data, and from one or two relatively obvious magnetic features appearing on more than one track, that the geological trend crosses the tracks at a wide angle. As far as can be checked from the form of the major anomalies with respect to the calculated regional base line, magnetization in the Earth's field direction can be assumed. Although it is rarely possible to isolate individual anomalies with certainty since the profiles consist of a series of peaks and troughs, it seems most probable that each major positive peak and its adjacent trough on the south side can be taken as representing the magnetic effect of a single body. It was found that these magnetic features could be approximately fitted by magnetic profiles calculated at right angles to flat-topped prism-shaped bodies which were assumed to extend indefinitely in a direction perpendicular to the magnetic meridian. This geometric form was therefore taken as a model for the shape of the bodies. From a statistical study of selected parameters of the major magnetic features (those with a well-defined maximum and minimum, and with a peak to peak amplitude of between 40 and 400 gamma), an attempt was made to obtain information about the variation in form and depth of the bodies. Clearly, the validity of this procedure depends on how closely the model approximates to actual conditions. For example, the model assumes indefinite lateral extent for the bodies, and thus takes no account of the fact that some tracks will be across bodies of limited length, nor that some tracks will cut across the flanks of anomalies rather than over their centres. However, if the anomalies have a tendency to be elongated, which is not uncommon, and if the structural trend is indeed across the tracks, as evidence suggests, then the model is probably acceptable.

The north–south magnetic profile across a body of the form chosen is shown in Fig. 27. Three measurements were taken as shown in the diagram. They are u, the peak to peak amplitude, v, half the horizontal distance between the points of half maximum gradient and w, the horizontal distance from the positive peak to the curve at half the vertical distance between peaks.

For a model assumed to be of infinite depth these quantities can be quite simply expressed in terms of the width, depth to top surface, and intensity of magnetization of the body. In order to simplify the calculation a field inclination of 45° is assumed, which is accurate enough for the purpose, as the actual inclination averages about 55° and so many variables are unknown that only rough calculations can be made.

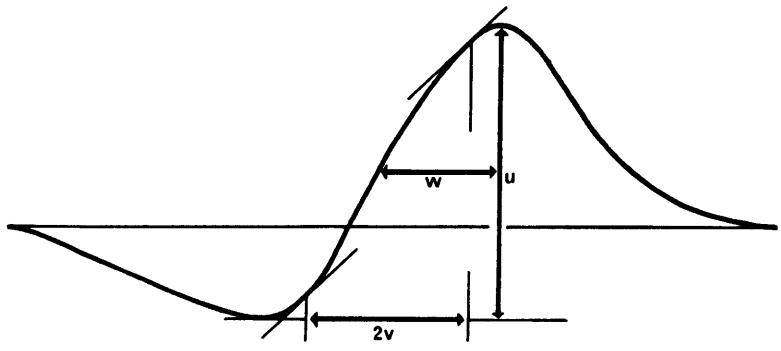

FIGURE 27
A magnetic feature showing the indices u, v and w.

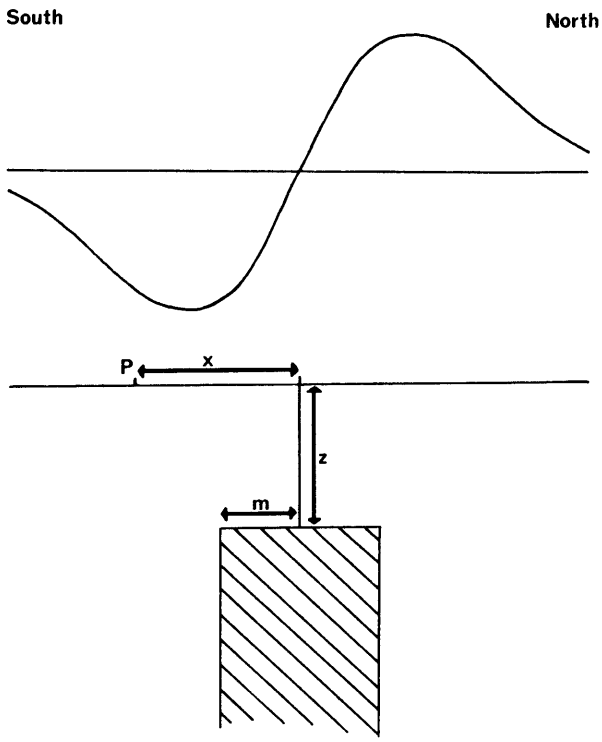

FIGURE 28
South–north section of the model (Fig. 27), showing the quantities x, z and m.

Referring to Fig. 28, if $x/z = n$, and $m/z = b$, then the total field anomaly at a point P is

$$T = J \ln \frac{(n+b)^2+1}{(n-b)^2+1}, \tag{1}$$

where J is the intensity of magnetization. By differentiating the expression with respect to n, and equating to zero, the following expression is obtained

$$n_w = (b^2+1)^{\frac{1}{2}}, \tag{2}$$

where $n_w = w/z$.

The horizontal distance $2v$ between the two points of half maximum gradient on the curve can also be expressed as a function of b. If $n_v = v/z$, then

$$n_v = [\{(b^2+1)^2+4\}^{\frac{1}{2}}-2]^{\frac{1}{2}}. \tag{3}$$

A simple graphical method of finding the points of half gradient is given by Peters (1949). A line is drawn tangent to the curve at its maximum gradient. A second line is then drawn with a gradient of half this value. Two further lines are now drawn tangent to the positive and negative portions of the curve. The horizontal distance between the points at which these touch the curve is the required distance. The ratio n_w/n_v is equal to w/v. Therefore, for any magnetic feature, by measuring the respective values of v and w the value of b can be determined. Hence, m and z are also found.

The maximum amplitude is

$$\frac{u}{2} = J \ln \frac{(b^2+1)^{\frac{1}{2}}+b}{(b^2+1)^{\frac{1}{2}}-b}. \tag{4}$$

If the bodies are assumed to be of finite thickness, the quantities u, v and w are not so simply expressed, but they can be easily obtained as a function of depth and width for a body of given thickness from measurements of a series of calculated and plotted anomalies.

It was noticed that there is a considerable area in the region studied where the separate graphs of u, v and w plotted against distance for each of the tracks show a quite obvious correlation (this can be seen, for instance, in Fig. 35, over the length of track marked B_1). In all there are 48 well-defined features in this particular area and the calculated correlation coefficients, r_{uv}, r_{vw} and r_{uw}, are significant. It was

also observed that there is a general decrease in amplitude of the features from west to east across the five tracks. If this "regional" trend in amplitude is removed by proportionally reducing the amplitudes of all the features so that the average for each line is the same, then the correlation between amplitude and depth indices becomes even more significant and is extremely unlikely to be due to chance (probability $p < 0{\cdot}001$).

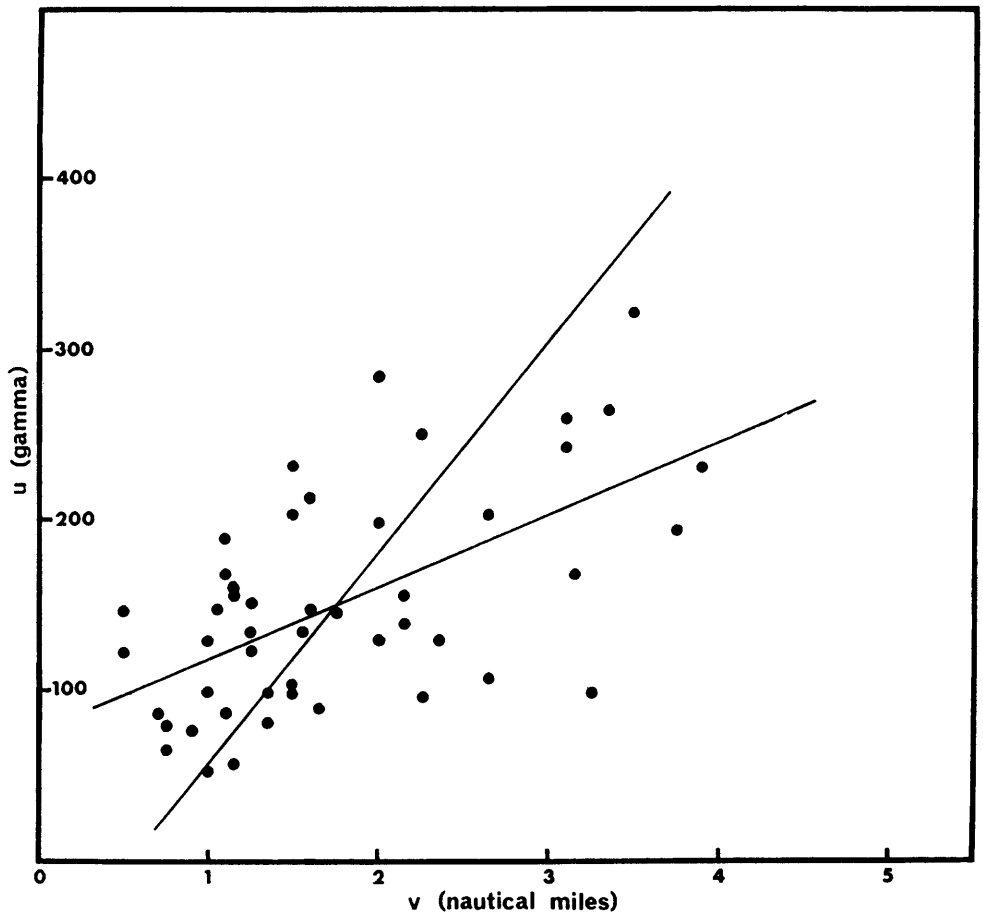

FIGURE 29

Plot of u against v for observed magnetic features in the Drake Passage area. u in gamma, v in nautical miles.

In Fig. 29 the corrected amplitudes are plotted against the appropriate values of v, together with the calculated regression lines. In Fig. 30 the relationships are plotted on a double logarithmic scale, so that the intensity of magnetization merely determines the positions of the regression lines and not their gradients. It is therefore possible, by plotting the relationships between u and v for changes in dimensions of various models, to determine which type of variation best simulates the observations. A number of these relationships are shown in the figure. The intensity of magnetization is kept constant in every case.

Line A shows the relationship for bodies of infinite transverse extent and infinite thickness, but varying in width. Lines E_1 and E_2 show the relationship when blocks of finite thickness are varied in width. Lines B and F show the very different variation (for bodies of infinite and finite thickness, respectively) that occurs when the width is kept constant and the depth is varied. Line C shows the change in amplitude and depth index due to a reduction in transverse length, and line D shows the effect of variation in thickness.

Variations of types A, C, E_1 and E_2 certainly fit the data, but those of types B, D and F do not. Those of types A, C, E_1 and E_2 represent variations in the horizontal dimensions, in the case of A and C of infinitely thick bodies, and E_1 and E_2, of bodies of finite thickness. In terms of either the finite or infinite model, the observations can therefore be explained in terms of variations in width or length of bodies

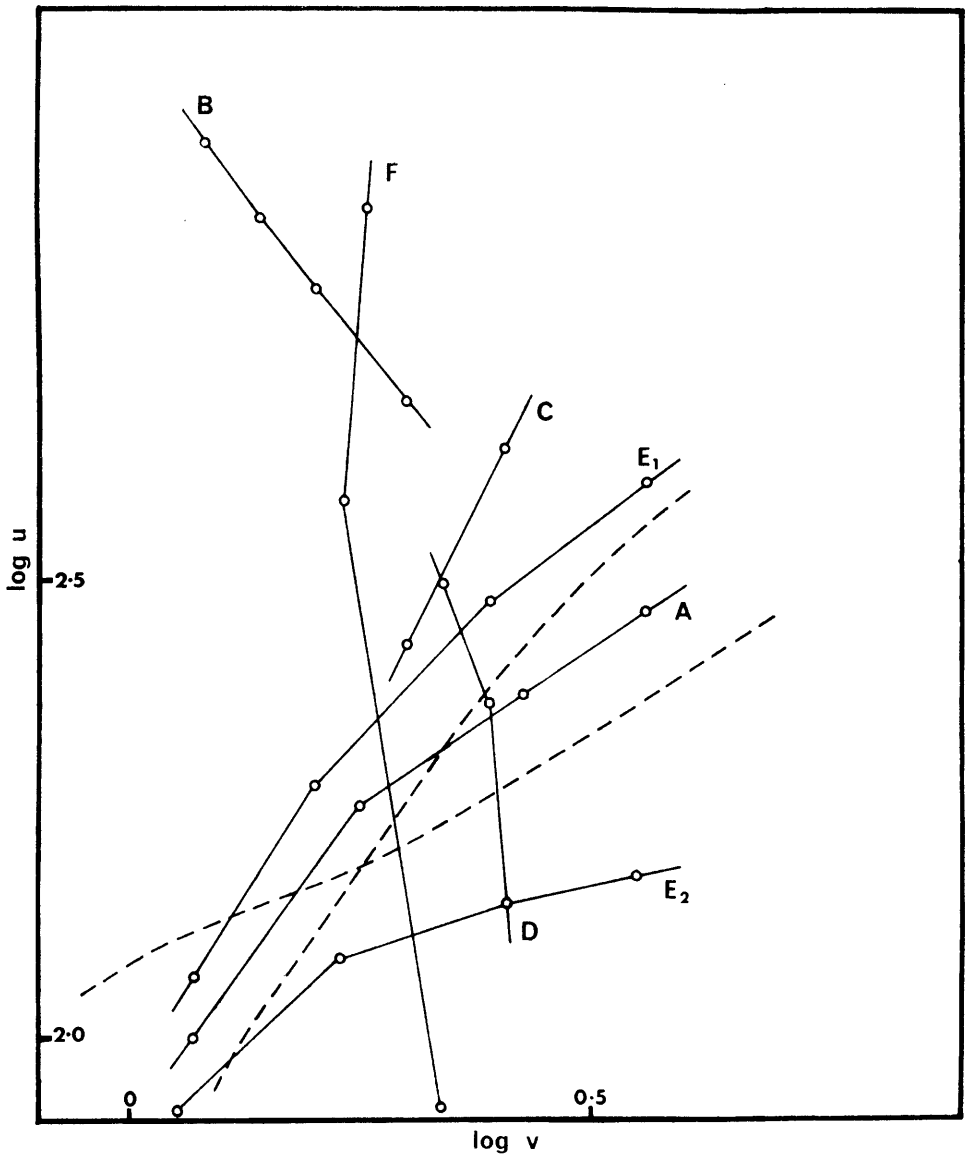

FIGURE 30

Plot of log u against log v. The regression lines of Fig. 29 are plotted as dashed lines.

Line	*Dimensions of Body (Limits of variable dimensions are given)*			
	Width along Profile	*Depth to Upper Surface*	*Transverse Length*	*Vertical Thickness*
A	2–8	2	∞	∞
B	2	2–4	∞	∞
C	2	2	12–∞	∞
D	6	2	∞	1–4
E_1	2–10	2	∞	2
E_2	2–10	2	∞	1
F	4	1–4	∞	1

Units are multiples of v.

at constant depth. The high correlation between amplitude, u, and "depth index", v, for the features along any one track suggests that the intensity of magnetization is relatively constant in a north–south direction. When all the data are considered together the improvement in correlation that results from adjusting the amplitudes points to a systematic increase in intensity in a westerly direction, though other explanations, such as a general increase in thickness of the blocks, are possible.

If depths and widths are now calculated from v and w, using equations (2) and (3), for a prism of infinite thickness and length, the average width is found to be 3·6 miles (6·7 km) and the average depth to be 2·7 km. Such a body would require an intensity of magnetization of $4{\cdot}5\times10^{-4}$ e.m.u./cm.^{3} to produce the average magnetic anomaly of 150 gamma. Alternatively, if a model of infinite length but 1·6 km. thick is used, the average width obtained is 3·0 miles (5·6 km.) and the average depth is 3·2 km., which is about equal to the sea depth. In this case the intensity of magnetization required to produce a 150 gamma anomaly is $1{\cdot}5\times10^{-3}$ e.m.u./cm.^{3}. When thinner models are considered, both their depths and intensities of magnetization must increase, a limiting condition being approached by a model 0·8 km. thick, 3·2 miles (5·9 km.) wide and at a depth of 3·6 km., which would require an intensity of magnetization of $3{\cdot}0\times10^{-3}$ e.m.u./cm.^{3}, a figure approaching that of strongly magnetized basic igneous rocks.

As it is unlikely that the bodies have an infinite length normal to the track direction, calculations based on this assumption are most probably subject to some error. It can be shown, however, that the limiting depth for bodies which are horizontally equidimensional is approximately 4·8 km.

To summarize the preceding arguments, it may be said that the observed correlation of amplitude and depth index can be simply explained as due to prism-shaped bodies of infinite, or finite but constant thickness, varying in horizontal dimensions and with upper surfaces all at about the same depth. Apart from a systematic regional change, the intensities of magnetization do not vary much from one body to another. An exact value for the depth to their top surfaces can only be given if the length and thickness of the prisms is defined, but from the above calculations it would appear to be less than 4·8 km., i.e. within 1·6 km. of the sea floor.

If the bodies are visualized ideally as being infinitely long blocks of 1·6 km. thickness with their upper surfaces at a depth of 3·2 km. as calculated above, then to achieve a comparable range of v and w to the observed range, the blocks must vary in width from 1·5 to 8·0 miles (2·8 to 14·8 km.). Similar blocks of thickness only 0·8 km. must vary from 2·0 to 9·0 miles (3·7 to 16·7 km.) in width. As the separation of observed positive peaks is in the range 10–20 miles (18·5–37 km.), the separation of individual blocks must be such that their anomalies interfere to some extent, though not usually enough to alter the values of u, v and w to an extent that would invalidate the analysis. In these circumstances it is found that by keeping the horizontal dimensions of the block constant and varying their spacings, a similar effect to that of varying the horizontal dimensions is produced. Fig. 31 shows an example in which identical

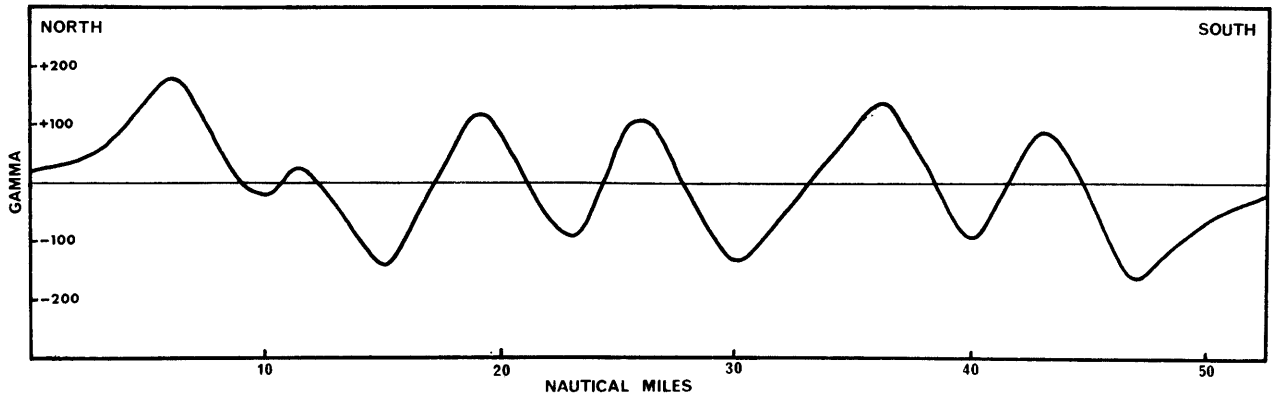

FIGURE 31

Total magnetic field along a north–south profile across a series of model blocks.

blocks of infinite length, 4 miles (7·4 km.) wide and 1·6 km. thick are separated by different distances. The resulting relationships between u, v and w are shown in Fig. 32. This is almost identical to that observed in the central area of Drake Passage, though it is of much smaller range. It is apparently necessary to vary

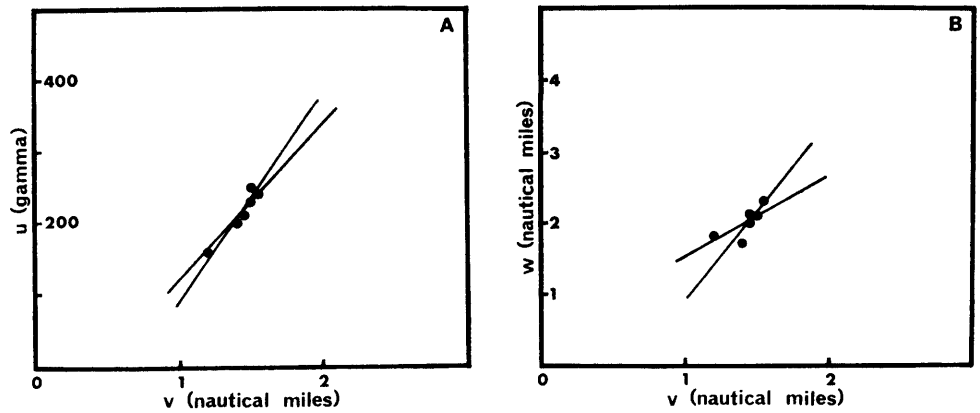

FIGURE 32

Plot of u against v (A) and w against v (B) for the magnetic profile of Fig. 31.

both the horizontal dimensions of the blocks and their separations to achieve a range comparable to that observed.

So far, it has been assumed that the blocks have vertical sides. This is, however, not a necessary restriction; indeed, sloping boundaries for thin blocks would seem to accord more with known geology and geomorphology. An infinitely long block of triangular cross-section with sides sloping at 8°, of height 1·2 km., with its apex just below the sea floor at a depth of 3·2 km., has an anomaly with v and w in the observed range, and would require an intensity of magnetization of 3×10^{-3} e.m.u./cm.^{3} to account for the average anomaly. However, if the distances apart of a series of such identical blocks is varied, it is found that, although v and w tend to show a relationship comparable to that observed, the range of values is very small because the blocks are so wide that their anomalies only interfere to a slight extent. To achieve this range a series of differing bodies at different distances apart must be present.

The relationships plotted in Fig. 33 are obtained from a series of such bodies with their apices at a depth of between 3·2 and 4·0 km. and with slopes of less than 9°. Widths at their bases range from

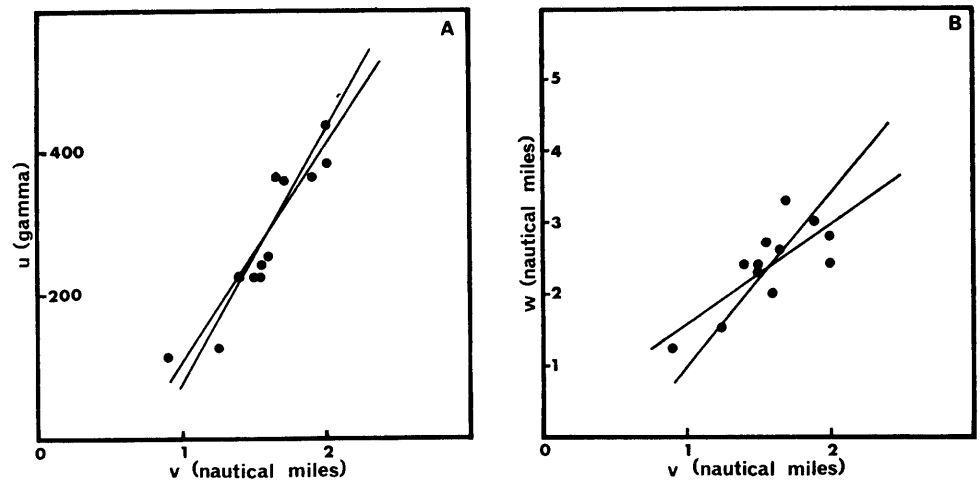

FIGURE 33

Plot of u against v (A) and w against v (B) for magnetic profiles across a series of blocks of triangular cross-section.

6 to 11 miles (11·1 to 20·4 km.) and heights from 0·8 to 1·2 km. This series also includes three bodies with double peaks that result from the coalescing of two single bodies. In this example the effect of length variations has not been considered but qualitatively it is the same as changes in width.

Although the possibilities of variation in form and grouping have not been exhausted, all the simple types have been considered. Furthermore, neither changes in angle of boundary slope nor changes in

dip of the blocks (unaccompanied by other types of shape variation) can account for the observed relationships. Thus, it seems valid to interpret the form of the magnetic features in this area as due simply to variation in horizontal dimensions and spacings of a series of bodies of similar shape lying at a shallow depth below the sea floor.

Nothing, however, can be deduced about the thickness of these bodies from the available data. If they are major intrusions within the ocean floor having a higher or lower intensity of magnetization than the "country rock", they are likely to be of great thickness and are comparable with the infinitely thick prisms of the model. Such a body, with a width of 3·6 miles (6·7 km.) and an anomaly of 150 gamma requires a contrast in intensity of magnetization with surrounding rocks of $4{\cdot}5\times10^{-4}$ e.m.u./cm.^{3}. Contrasts of this magnitude between known types of basic intrusive igneous rocks are quite reasonable.

An alternative possibility is that the anomalies are at least partly caused by the topography of basic igneous rocks, which may be either lavas extruded on the ocean floor or part of the original crust. As there is in general no obvious relationship between the magnetic features and the observed bottom topography, it has to be presumed that the solid rock is in many places buried by sediment. If the triangular blocks are conceived as representing the topography, then a contrast of magnetization intensity of 3×10^{-3} e.m.u./cm.^{3} is required. This would suggest that the rock is basic in character and that it has a marked remanence. To obtain a reduction in the remanence it is necessary to increase the topographic range, which means increasing the slopes. From measurements of slopes of observable marked features on the ocean bottom, values much greater than 10° seem to be generally unlikely. In one of the few places where it seems possible to account for an observed magnetic feature by topography a fairly good agreement was obtained between the calculated and observed anomalies when an intensity of 5×10^{-3} e.m.u./cm.^{3} was used. The topography was supposed to extend indefinitely in a direction perpendicular to the track, the magnetization being in the field direction. Recent measurements made by Ewing and Engel (1962), and Heezen (1962) with a seismic profiler in other oceanic areas show that sub-bottom topographic relief of the magnitude required is present.

No doubt the actual geological conditions are more complicated than outlined above. Both topography and lateral changes in intensity of magnetization, such as are produced by intrusion, are likely to occur, but to produce the observed correlation between u and v it is necessary for one or other to predominate unless the two effects are interrelated.

There are other geological conditions which might bring about the necessary lateral changes in intensity of magnetization. For example, the alternating thin blocks of magnetic and relatively non-magnetic material might be piles of lavas from different vents, where there is a considerable contrast in the average magnetization of the lavas from each vent. Although such a possibility cannot be dismissed, it seems unlikely that such complex geology would produce a relatively simple magnetic picture. Also, if the lavas lie in valleys, as suggested by Mason (1960), then the "country rock" must be relatively non-magnetic, contrary to what is usually supposed for the crust in an oceanic area.

2. *Correlation of magnetic profiles*

Apart from the obvious correlation between u, v and w observed on a number of profiles in an area of Drake Passage, it was noticed that along certain lengths of profile in other areas less obvious but nevertheless definite relationships existed between u, v and w. This suggested a possible method of correlating profiles. The technique finally used has already been described by Griffiths and Riddihough (1963) but a more detailed account of it is given below. It is still too early to be sure that the method in its present form is a valid one. This can only be established by testing it as more data are collected.

For each track three separate graphs are drawn showing the variation of u, v and w with distance, and two ancillary graphs of the changes $\delta u/\delta v$ and $\delta w/\delta v$ with distance, where δu, δv and δw are the differences along the tracks between consecutive values of u, v and w. The use of a third possible relationship, the variation of $\delta u/\delta w$ with distance, has been found to be superfluous, because in practice it provides no additional information of value.

The division of the tracks into sections is done by inspection in the following way. Over certain lengths of track there is an obvious similarity in the variation of the three indices; over other track lengths only two indices may show any visible correlation and there are also stretches where all three indices are apparently unrelated. The points at which changes in the nature of these mutual relationships occur are taken as boundaries. Although most of the main divisions can be made by careful inspection

of the graphs of u, v and w, the two subsidiary graphs are used where possible to assist their recognition. Unfortunately, one or more of the quantities δu, δv and δw is sometimes so small that $\delta u/\delta v$ and $\delta w/\delta v$ become indeterminate and thus of no help.

The division into groups having been visually established, the probability levels of the correlation coefficients r_{uv}, r_{vw} and r_{uw} for each section of track are determined. These levels are used to classify the sections into the types listed in Table IV.

TABLE IV

Type	*Probability Levels of Correlation Coefficients*		
	<10 per cent	10–15 per cent	>15 per cent
B_1	$r_{uv}r_{vw}r_{uw}$		
B_2		$r_{uv}r_{vw}r_{uw}$	
OR	any two		
C_1	r_{vw}		$r_{uv}r_{uw}$
C_2		r_{vw}	$r_{uv}r_{uw}$
D_1	r_{uv}		$r_{vw}r_{uw}$
D_2		r_{uv}	$r_{vw}r_{uw}$
E_1	r_{uw}		$r_{uv}r_{vw}$
E_2		r_{uw}	$r_{uv}r_{uw}$
F			$r_{uv}r_{vw}r_{uw}$
A_1	No magnetic features.		
A_2	Less than one feature per 75 miles (140 km.)		
G	Areas of very narrow magnetic features of high frequency per mile (confined to shallow-water areas).		

Finally, note is taken of any characteristic of the groups, e.g. particular patterns of variation, rises in average value, etc., which might aid correlation between tracks or necessitate a further sub-division of the tracks. The various tracks, plotted in their proper positions and divided into sections, are then inspected. Where appropriate the boundaries are extended from one track to another, thus defining regions of different magnetic type.

It must be emphasized that this method does not depend on the various correlation coefficients reaching a high level of significance. Probability levels merely serve to define magnetic types and it is the various types which are used in correlation from profile to profile. The numerical values of the probability levels, i.e. 10 and 15 per cent, were chosen from observations so as to give a wide range of types in the area studied. However, it may well be that in the light of experience these probability levels will have to be revised. There is already some evidence to suggest that the system of classification may have to be simplified and the number of types reduced.

To illustrate the use of this technique three tracks from the Drake Passage area, where the water depth is fairly constant at about 2,000 fathoms (3,660 m.), have been taken as examples. These are given in Fig. 34. They trend approximately north to south in direction and are numbered 1, 2 and 3 from east to west. Apart from the magnetically undisturbed area in the north, these tracks show no obvious features which can be used for correlation. The values of u, v, w, $\delta u/\delta v$ and $\delta w/\delta v$ for the three tracks are plotted in Figs. 35, 36 and 37.

On track 3 the most noticeable feature in the graphs of u, v and w is an easily defined section of type A between 50 and 250 miles (95 and 465 km.) south of Port Stanley. South of this u, v and w show

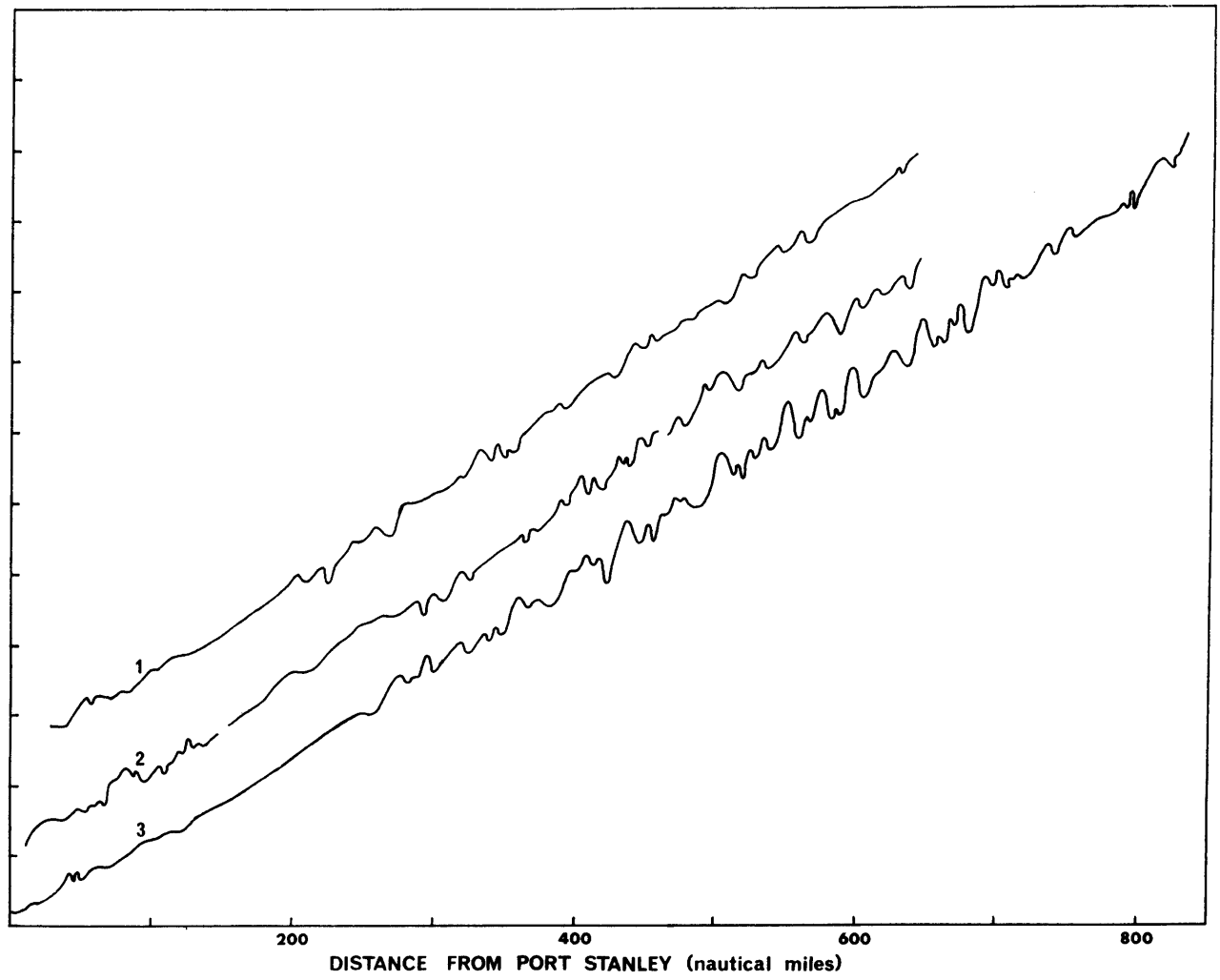

FIGURE 34

Total magnetic field profiles across Drake Passage plotted relative to arbitrary base lines. Intervals on the vertical axis are 10^3 gamma.

a recognizable correlation until the area around 550 miles (1,020 km.), where there is a sharp rise in u, v and w. The rise in average value of u at this point continues southward but it is not followed by v and w. At 685 miles (1,270 km.) u drops in value again and the correlation between u, v and w becomes stronger. From the graph of $\delta w/\delta v$ it can be seen that the track from 250 to 320 miles (465 to 585 km.) is different in character from that south of 320 miles (585 km.). From the gradient graphs it is possible to isolate an area between 510 and 580 miles (945 and 1,075 km.) which apparently represents a transition zone on the u, v, w graphs centred at 550 miles (1,020 km.). The final positions of the divisions moving southwards are thus: 50 and 250 miles (95 and 465 km.), bounding an area of no magnetic features; 320 miles (585 km.), at a change in character shown most clearly on the $\delta w/\delta v$ graph; 510 and 580 miles (945 and 1,075 km.), bounding an anomalous area on both the $\delta w/\delta v$ and $\delta u/\delta v$ graphs and containing another division at 545 miles (1,010 km.) which marks an increase in u; and 685 miles (1,268 km.), at a drop in value of u and a return of the close correlation between u, v and w. Calculation of the correlation coefficients determines the types illustrated in the graphs.

Track 2 shows the A-type section between 125 and 200 miles (230 and 370 km.). Beyond this point there is no close correlation between the graphs of u, v and w, and there are no obvious major changes until 495 miles (915 km.), where there is a sharp feature on all three graphs and a rise in average value of v. The graphs of $\delta u/\delta v$ and $\delta w/\delta v$, apart from one high value at 325 miles (600 km.), enable an anomalous area to be defined between 390 and 430 miles (720 and 800 km.). A further division at 490 miles

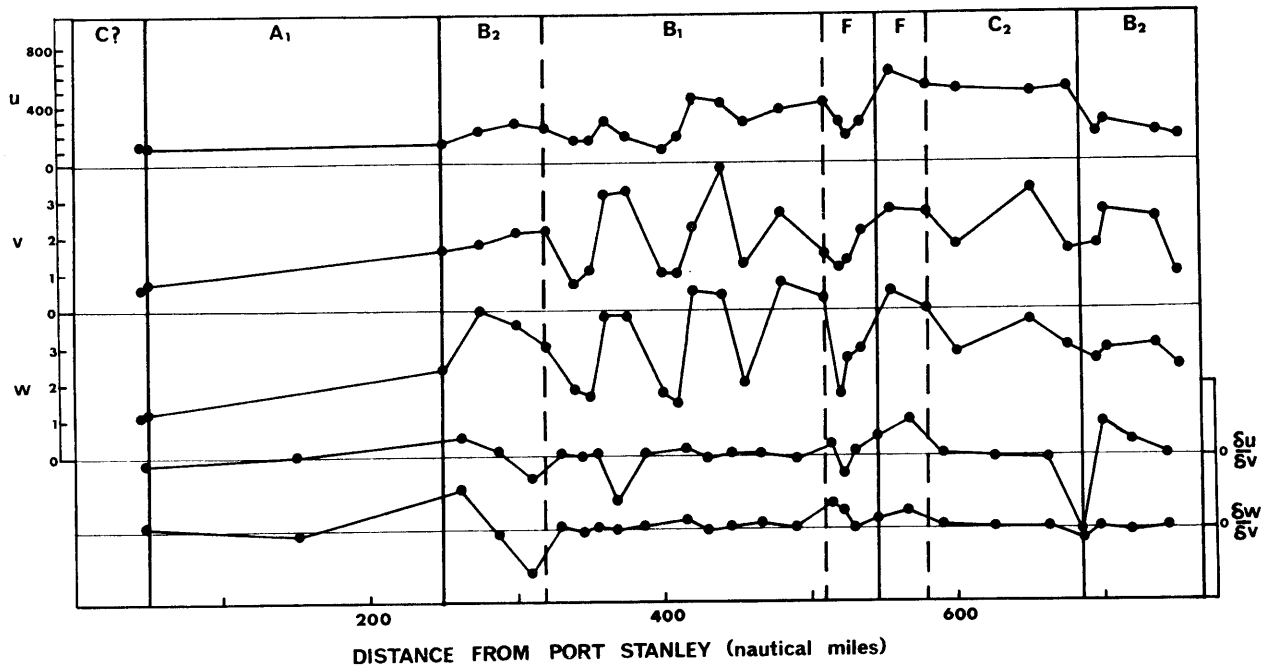

FIGURE 35

Plots of u, v, w, $\delta u/\delta v$ and $\delta w/\delta v$ against distance for track 3. The vertical dividing lines are of two types: solid when obtained from inspection of the u, v and w graphs, and broken when obtained from inspection of the graphs of $\delta u/\delta v$ and $\delta w/\delta v$.

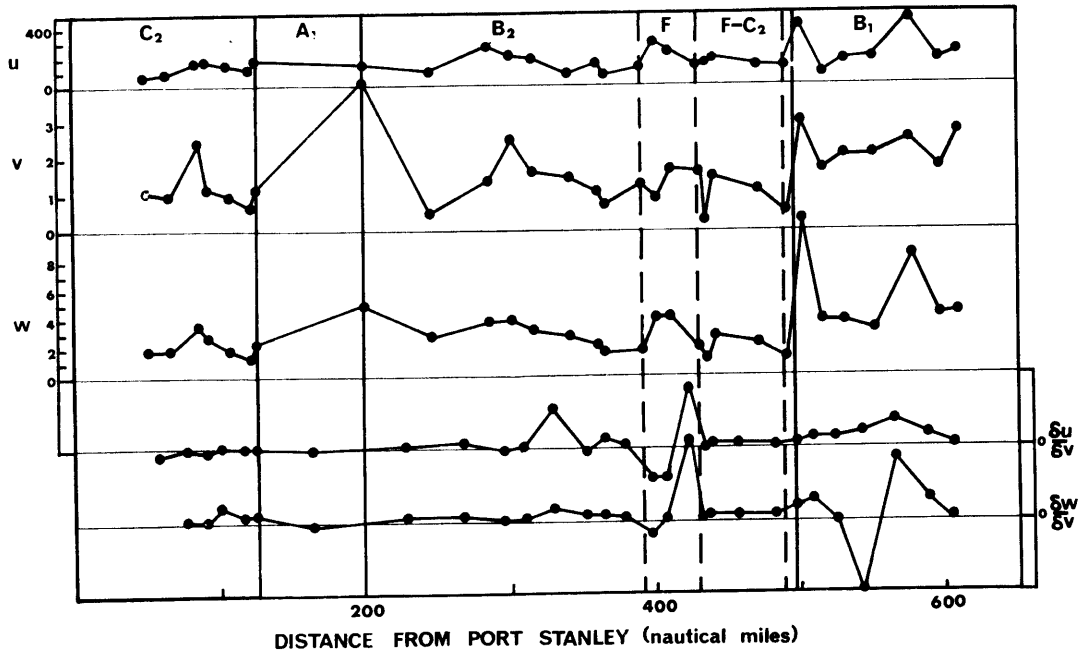

FIGURE 36

Plots of u, v, w, $\delta u/\delta v$ and $\delta w/\delta v$ against distance for track 2. The vertical dividing lines are of two types: solid when obtained from inspection of the u, v and w graphs, and broken when obtained from inspection of the graphs of $\delta u/\delta v$ and $\delta w/\delta v$.

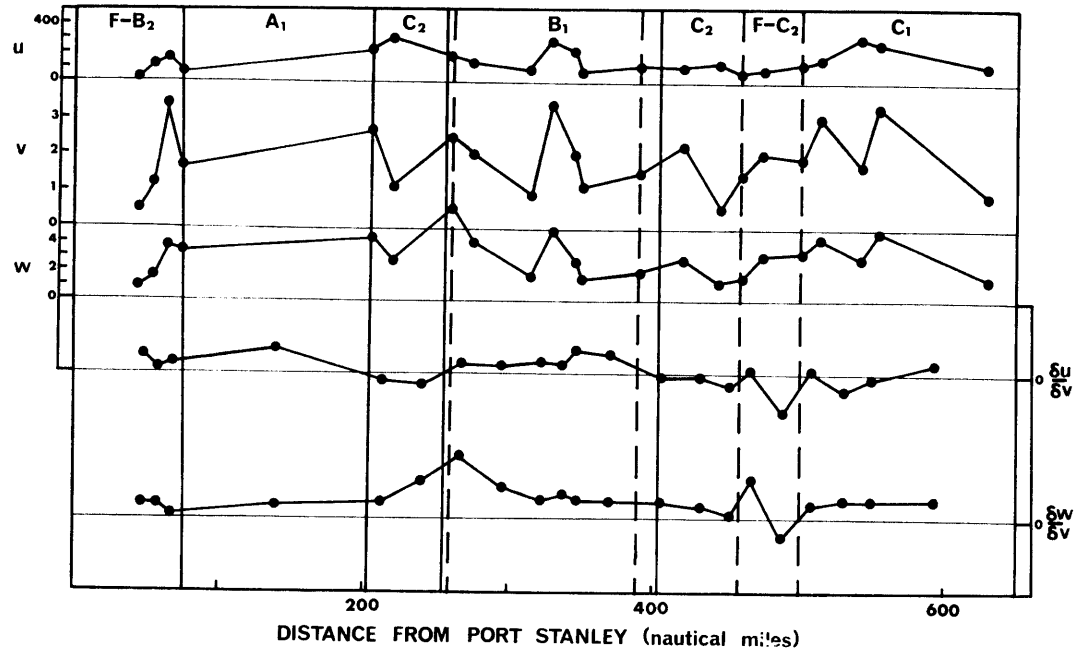

FIGURE 37

Plots of u, v, w, $\delta u/\delta v$ and $\delta w/\delta v$ against distance for track 1. The vertical dividing lines are of two types: solid when obtained from inspection of the u, v and w graphs, and broken when obtained from inspection of the graphs of $\delta u/\delta v$ and $\delta w/\delta v$.

(790 km.) is shown on both these graphs. Farther southward the divisions are: 125 to 200 miles (230 to 370 km.), bounding a non-magnetic area; 390 to 430 miles (720 to 800 km.), from the graphs of $\delta u/\delta v$ and $\delta w/\delta v$; and 490 miles (910 km.) from all five graphs. Investigation of the statistical correlations of the groups introduces a few minor variations, in particular the isolation of a small area between 200 and 210 miles (370 and 390 km.) which contains one highly anomalous measurement. Between 210 and 390 miles (390 and 720 km.) only the correlation coefficients of v/w and u/w reach significance, thus placing this area in the B_2 type. The area between 430 and 490 miles (800 and 910 km.) is statistically of F type, but by inspection it is closely related to the C type. South of 490 miles (910 km.), the category is B_1.

Track 1 shows an easily defined A-type area between 75 and 205 miles (140 and 380 km.). Between 205 and 255 miles (380 and 470 km.) correlation between v and w is close but between u at both v and w there is an almost inverse correlation. Between 255 and 405 miles (470 and 750 km.) correlation between u, v and w can be seen from the graphs. South of this the variations in v and w bear no relation to those of u. The graph of $\delta u/\delta v$ confirms a division at 260 miles (480 km.), where there is a change from positive to negative values, and also shows another at 390 miles (720 km.), where there is a further change to a dominantly negative average value. The graph of $\delta u/\delta v$, apart from a peak at 265 miles (490 km.), is extremely constant in character except between 460 and 500 miles (850 and 925 km.). The divisions obtained are now: 75 and 205 miles (140 and 380 km.), bounding a non-magnetic area; 205 to 210 miles (380 to 390 km.) and 390 to 405 miles (720 to 750 km.), determined from all five graphs; and 460 to 500 miles (850 to 925 km.), from the graph of $\delta w/\delta v$. These categories have been obtained statistically and the F type between 460 and 500 miles (850 and 925 km.) is again very closely related to the C type.

Correlation between these three tracks is shown diagrammatically in Fig. 38. The area of type A_1 is well defined on each track, and is bordered to the north by areas which are somewhat indeterminate due to the lack of data. To the south all three tracks cross a B-type area, though there is a small section of C type on track 1. The B area is bounded in the south by an F area on tracks 3 and 2 but by a C_2 area on track 1. Divisions here are more complex, though it can probably be assumed that an F type with a dominant probability of C type will grade into an area where the C correlation becomes significant. The sudden rise in amplitude at 545 miles (1,010 km.) on track 3 may be correlated with a

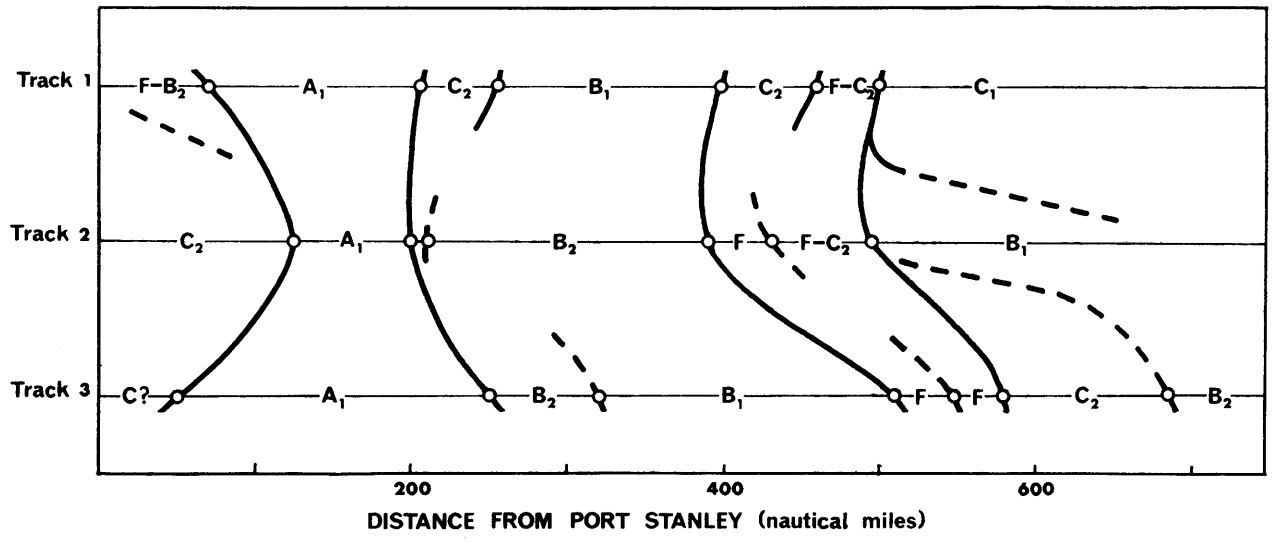

FIGURE 38

Diagram showing the correlation between tracks 1, 2 and 3.
——O—— Type boundary.
— —O— — Division of degree within one type or type boundary of uncertain position.

similar feature at 495 miles (915 km.) on track 2 and again at 500 miles (925 km.) on track 1, though it is clear that it would not coincide always with the same division of type. The southern parts of all tracks have very little in common, and this is provisionally interpreted as indicating that boundaries of type run almost north to south rather than approximately east to west as in the northern parts of the region. In fact, it may well be that this area is structurally complicated and that the correlation technique breaks down here. The Drake Passage area on the final map (Fig. 39) is essentially the same as the diagrammatic map (Fig. 38) and is only slightly modified by data from another track between tracks 3 and 2, and by divisions made at the ends of the tracks from examination of the original records. Further tracks which are shown on Fig. 25 continue the divisions obtained from tracks 1, 2 and 3, and give further support to their validity.

It is only necessary to discuss these three tracks here. They are quite typical and are not tracks on which the divisions are particularly clearly marked. The method used for the construction of Fig. 39 is identical to that described above.

3. *Significance of the various magnetic types*

The divisions into the groups that have been obtained are based on the statistical similarity of a series of sections of magnetic anomalies. To some extent the shape of these sections depends both on the direction of the track crossing the anomalies and the orientation of the disturbing bodies with respect to the Earth's magnetic field. If a set of tracks is parallel or nearly parallel, then one of these variables is eliminated. In such circumstances magnetic features of a particular type, irrespective of which track they occur on, are likely to be caused by bodies of similar type, depth and orientation. It should be noted, however, that a change in type may well be produced by a systematic change in orientation of the bodies with respect to the tracks as well as, or instead of, a systematic change in the shape or depth of the body.

If tracks that are not parallel are now considered, there is clearly some doubt whether or not a particular type, say *B*, on an east–west track is equivalent to a type *B* on a north–south track. Fuller investigation of this problem is necessary, but at this stage it is perhaps useful to note the following points:

i. Elongated bodies with a north-east to south-west orientation, if crossed by east–west and north–south tracks, will exhibit approximately the same section.

ii. Horizontally equidimensional anomalies can be crossed at a wide range of angles without affecting the proportions of the sections greatly.

iii. Over a wide range of track directions amplitude values will not be much affected by changes in orientation of tracks across an anomaly, provided the peak is traversed.

Clearly, sections which are more nearly parallel to the elongation of a set of anomalies will show numerically greater values of v and w than other sections, but it seems likely that the degree of correlation is not dependent to any great extent on the angle of the track over a wide range of angles. Although any significant change in the values of v and w along any one track has been noted on this track and a division made, sections of one type on one track have been correlated with sections of the same type on other tracks which are not parallel, even though the average values of v and w may not have been the same on both.

Some confirmation of these assumptions is obtained from a set of north–south tracks measured in the area between the Falkland Islands and South Georgia which has already been crossed by five tracks with a dominant west-north-west to east-south-east trend. Despite the 80° difference in direction between the two sets of tracks, correlation coefficients for a set of values of v and w taken in the same area, but from two sets of data, show the same significance.

From the considerations given in the section on analysis, it can be assumed (with the reservations noted above) that each type, i.e. *B*, *C*, *D* and *E*, represents some specific form of variation in the parameters defining the bodies producing the anomalies. For instance, it has been shown that in areas of *B* type there are strict limits on the depth to the upper surface of the disturbing bodies and the variation in their intensities of magnetization, the main variations being in horizontal dimensions. Where u has little or no relation to v or w (type *C*), the intensity of magnetization of the bodies or their orientation may vary considerably, for variations either in depth or width alone should show as a well-defined relationship between amplitude and v and w. Again, type *C* may also represent simultaneous variation of depth and width with no dominance of either. *D*, *E* and *F* types are not widespread in this area but they may represent some other simple types of variation, although calculations carried out so far have given little indication of any conditions in which v and w are not closely related.

The very fact that statistically defined magnetic groups can be set up may therefore be taken as evidence for the presence of areas of relatively uniform geological type. However, it is not necessarily true that the boundaries of these areas are parallel to structural trends, but it is perhaps likely that they are. Where it has been possible to check structural trends, either by the correlation of magnetic features across tracks or by bathymetry (on the assumption that this is related to geology), it has been found that in seven out of ten observed cases the trends *do* run parallel to the boundaries drawn.

The geological significance of the *B*-type area has already been discussed, but it is felt that discussion of how the other types originate would be too speculative at the moment to be of value.

4. *Description of the magnetic type map*

The resulting magnetic map of the Scotia Sea and Drake Passage is given in Fig. 39.

South of the Falkland Islands a strongly defined belt of type *A* trends eastward from Tierra del Fuego. The southern boundary of this area appears to be strongly faulted at one point, as shown both by a displacement of the boundary of approximately 30 miles (56 km.) in a north-north-east to south-south-west direction and the occurrence of a small area of type *C* extending south-south-west from the boundary. The presence of this fault is further supported by bathymetric data.

Southwards, the bathymetry indicates a dominant north-east to south-west trend which is paralleled by the boundaries of the magnetic type areas. It is interesting to note that the north-east to south-west belt of type F—C_2 corresponds to "a belt of massive solidified volcanoes and block faults" postulated by Zhivago (1962). At approximately lat. 60°S. there is an east–west boundary which appears on at least three tracks and which could possibly be interpreted as a major fault. On track 3 (Fig. 35) this boundary coincides with a sharp increase in amplitude, and this is true to a lesser extent on other tracks to the east (tracks 2 and 1). The amplitude map (Fig. 40) also shows a high corresponding to this position. South of this inferred fault, boundaries appear to have swung round to become almost north–south.

Between long. 60°W. and South Georgia the belt of type *A* has an easterly trend but it narrows very considerably at long. 48°W., then swings to an east-south-east direction and continues to South Georgia. To the north of this area magnetic types are not generally well defined, except around long. 49°W. where short additional north–south tracks (not shown in Fig. 25) confirm the presence of a *B*-type area. The

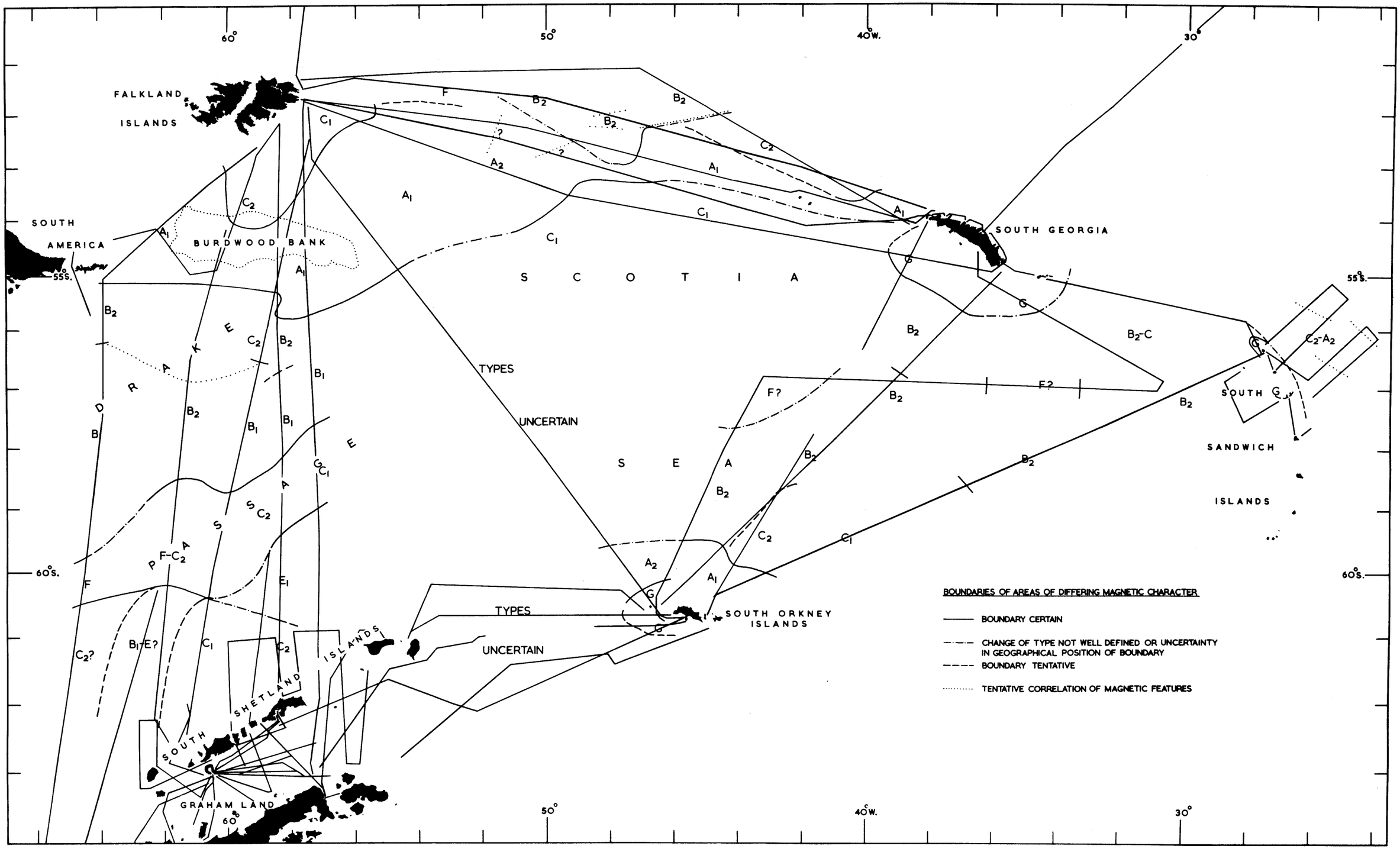

FIGURE 39

Map of the Scotia Arc showing magnetic types and boundaries (in red). The main magnetic traverses are shown in black.

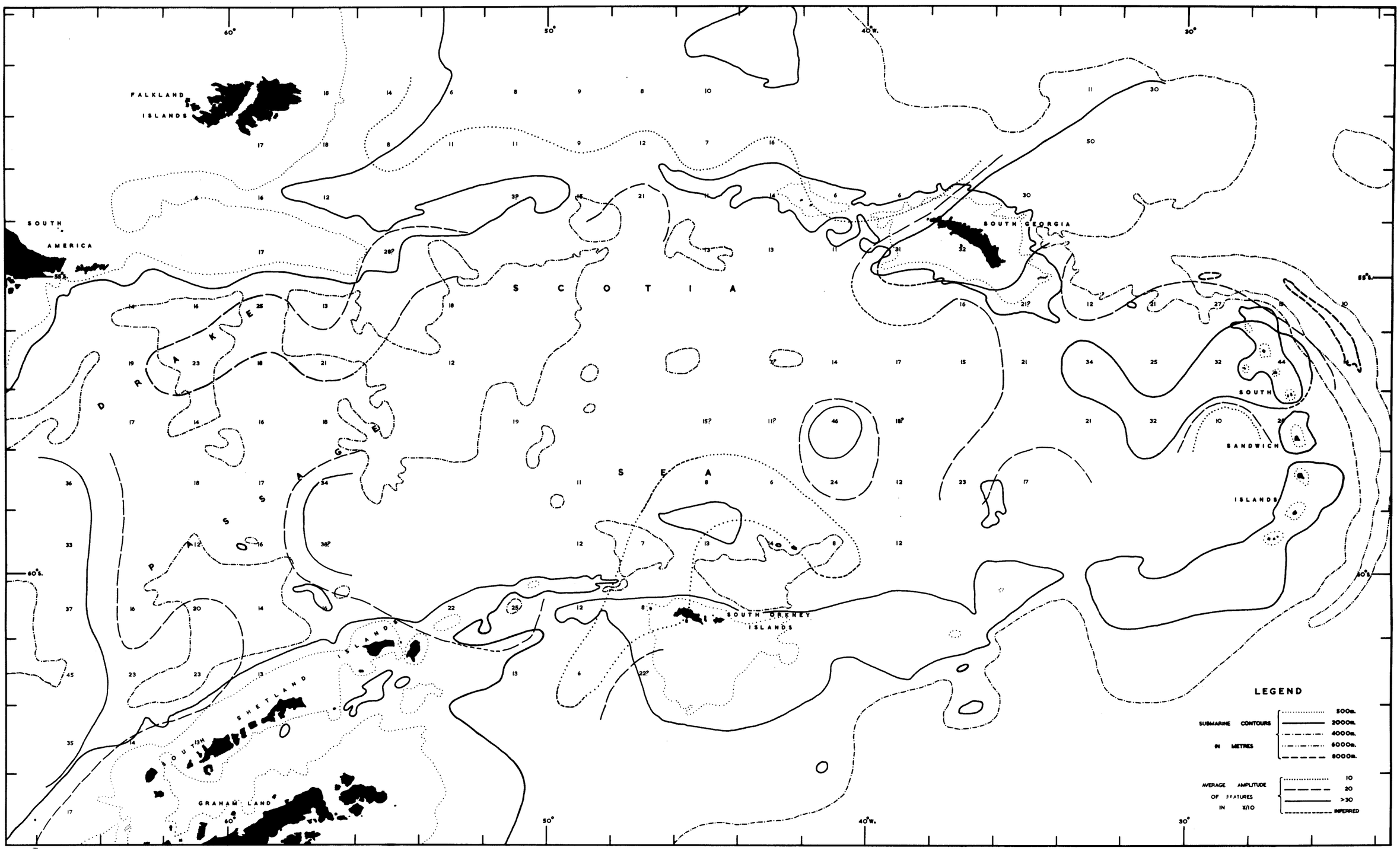

FIGURE 40

Map of the Scotia Arc showing contours of average amplitude of magnetic features calculated for 60 mile (110 km.) squares (in red). The contour interval is 100 gamma. The base map (black) shows the bathymetry.

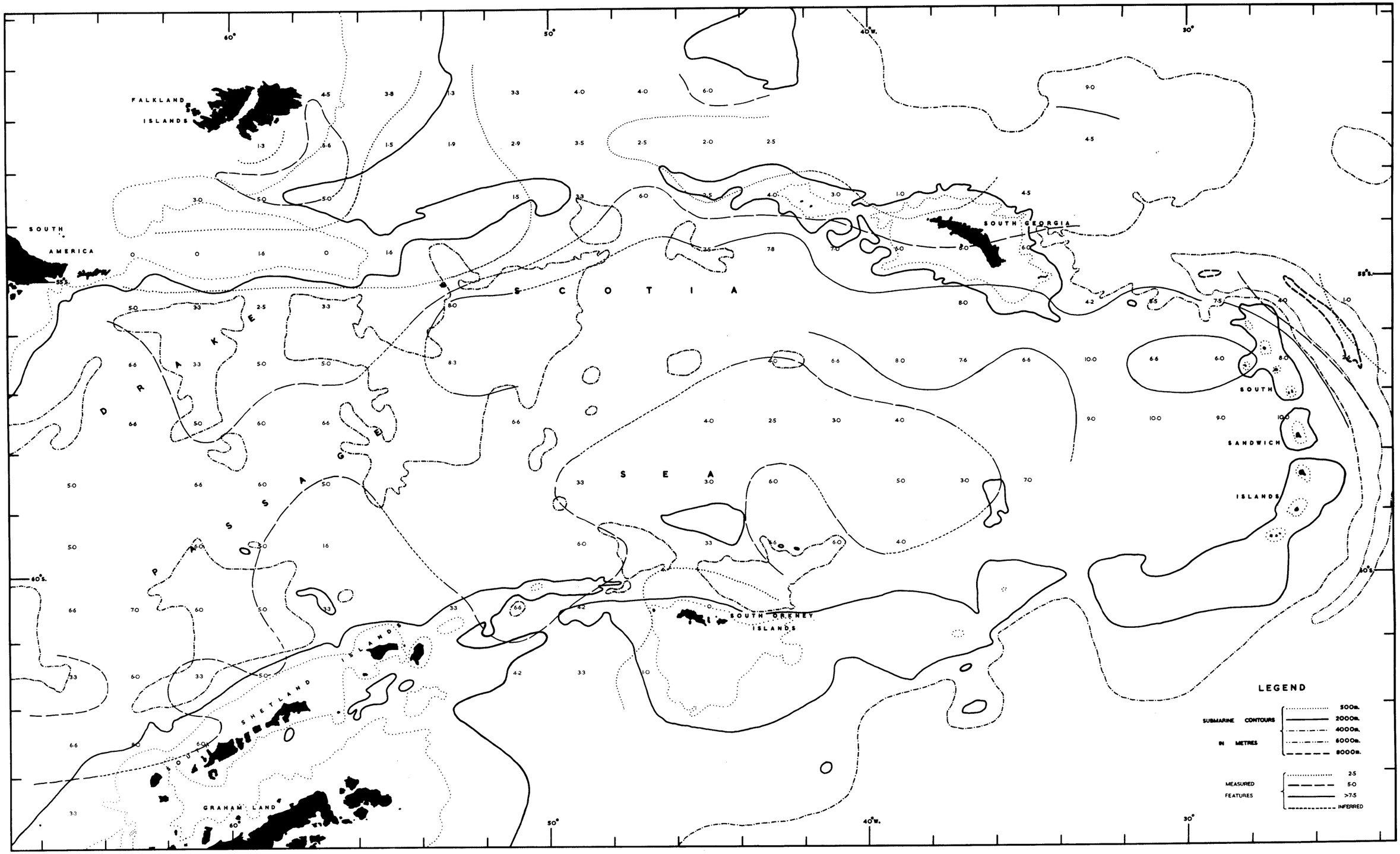

FIGURE 41

Map of the Scotia Arc showing the number of measured magnetic features per 100 track miles (185 km.) averaged for 60 mile (110 km.) squares (in red). The base map (black) shows the bathymetry.

tentative correlation of magnetic features, which occur on two adjacent tracks and coincide with the type divisions on the *u*, *v* and *w* graphs, suggests a possible fault in an east-north-east to west-south-west direction. Similar data were not obtained on any track to the west and therefore the presence of such a fault must remain speculative. It is interesting to note that in this area magnetic features usually do not have a close relation to the type boundaries which have been drawn.

Though data are limited in the area between South Georgia, the South Orkney Islands and the South Sandwich Islands, it is clear that the belt of type *A* does not continue east of South Georgia. There is some evidence to suggest that a northward extension of type *B* (from the few tracks observed) appears to form much of the sea floor to the south and passes between South Georgia and the South Sandwich Islands.

Much of the data in the central area cannot be easily correlated at this stage; however, it is apparent that this area is of greater complexity and variety compared with Drake Passage.

The South Sandwich Islands are highly magnetic and amplitudes of over 1,000 gamma have been recorded in their vicinity. The area to the east, over the trench, is of *C* type but with such a low frequency of anomalies per mile that it can be considered to be type C_2—A_2; however, from sections of comparable depth to those on the west of the islands, it is evident that the relatively non-magnetic character of this area is real and not an effect of water depth. There is no particularly characteristic anomaly associated with the trench and the anomalies that are present give depth estimates to the upper surface of the disturbing bodies not much greater than the sea depth.

Between the South Orkney Islands and the Elephant and Clarence Islands group, type boundaries appear to trend east-north-east to west-south-west; they intersect the tracks at a very small angle and are consequently very uncertain.

5. *Amplitude and frequency of magnetic features*

The amplitude of a magnetic anomaly depends on such factors as the size, depth and intensity of magnetization of the body producing it, variation in these factors being due to changes in geological structure and lithology. Although amplitude is therefore dependent on the variation of several factors rather than one, it was felt that on a regional scale average amplitude changes might afford some information about the geology of this area. Fig. 40, a contour map showing average amplitudes, has been prepared by dividing the whole area into 110 km. squares and averaging the peak to peak amplitudes of all the magnetic features in each square.

In Fig. 41 is plotted the frequency of occurrence of magnetic features in each square, omitting those with an amplitude of less than 40 gamma. This map is really a measure of magnetic activity and hence it is to some extent also related to the geology. In Figs. 40 and 41 the contours have a simple form, which points to the fact that the variations are not just statistical fluctuations. (A statistical study of amplitude variation in Drake Passage showed that an east–west change is highly probable.) It is interesting to compare these two maps (Figs. 40 and 41) with Fig. 39 to see whether or not the boundaries which it shows are confirmed, and if they are, whether Figs. 40 and 41 provide any additional information.

The amplitude map (Fig. 40) shows a clear eastward extension of the northern limb of the arc, defined by a belt of medium amplitude, lying between an area of low amplitude to the north and a less well-marked zone of higher amplitude to the south. There is no suggestion of the continuation of this belt from South Georgia to the South Sandwich Islands, but there is a possibility that it swings round south of South Georgia towards the South Orkney Islands. If this continuation is real, it marks the western edge of an area of high amplitude extending eastward as far as the South Sandwich Islands. Other features of interest are the region of high amplitude north of the South Shetland Islands and the extensive low-amplitude area in the vicinity of the South Orkney Islands.

The general trend of the contours on the frequency map (Fig. 41) is somewhat similar to that of Fig. 40. The northern limb of the arc is defined by a belt of low frequency which does not swing round southwards with the arc. The high-amplitude area west of the South Sandwich Islands is, as might be expected, one of high magnetic activity. Its eastern edge follows round the outside of the arc and the Meteor Deep, and farther to the east is a region of very low activity.

The amplitude low to the north of the South Orkney Islands appears to be an area of moderate activity, whereas Drake Passage is one of high activity.

Since the amplitude and frequency maps are obtained by an averaging procedure applied over 110 km. squares, it is obvious that only major regional changes in the magnetic anomaly field will show. Fig. 39

shows far more detail and therefore enables boundaries to be fixed with far more accuracy. Some features, such as those on the northern limb of the arc, are clear on all three maps. The type divisions of Fig. 39 do not, however, take account of amplitude variations or frequency of occurrence of anomalies and hence these maps show certain features which would not otherwise be apparent. Furthermore, to some extent at least, amplitude and magnetic activity bear a definite relationship to geology, whereas the geological significance of the areas of various magnetic types shown in Fig. 39 is not yet understood.

D. Bransfield Strait

The magnetic field in Bransfield Strait and adjacent areas has a complicated form, but when the field is smoothed and the regional gradient is removed a simple anomaly pattern emerges (Fig. 42). The smoothed values on which the contours are based were obtained by averaging and then removing a regional gradient of 14 gamma/nautical mile (7·7 gamma/km.). This value was derived from traverses made in the southern part of the Scotia Sea. The area is dominated by what is virtually one large anomaly consisting of an elongated high with an amplitude of over 800 gamma to the north of the South Shetland Islands, and a wider but shallower trough extending over most of Bransfield Strait. There is also a narrower, steeper, positive anomaly lying to the west of the trough and this appears to be a subsidiary peak of the main anomaly. Fig. 43 includes a section across the anomaly along the same line as that of the gravity anomaly. Inspection suggested the magnetization direction is about the same as the Earth's field so this direction was used in all attempts at interpretation.

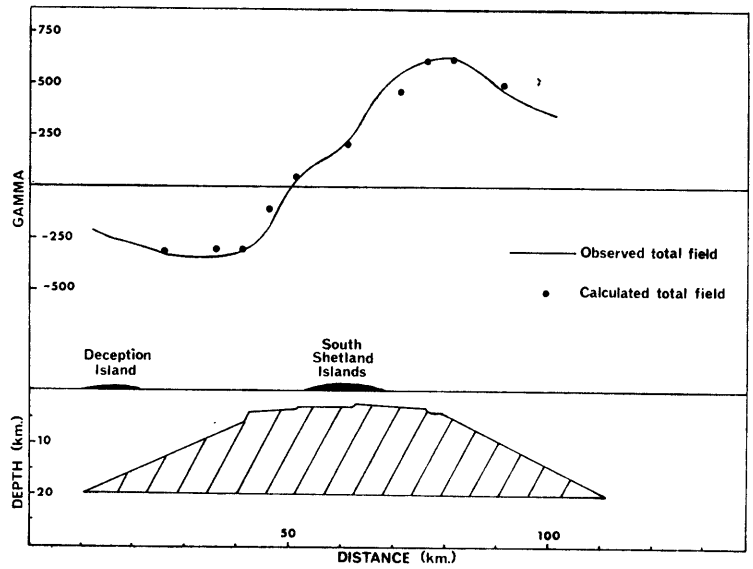

Figure 43

Magnetic profile and interpretation across Bransfield Strait. The line of section is AB in Fig. 19. The inclination of magnetization is assumed to be 58° and the susceptibility contrast approximately 6×10^{-3} e.m.u./cm.^{3}.

The anomaly is sufficiently elongated for a simple interpretation to be carried out, without too great an error, by assuming that the body producing it is of infinite length. An anomaly of such magnitude is likely to be due to a mass of basic igneous rock which will also have a high density. The reasonable supposition was made that the highest density layer shown in Fig. 24 is the rock producing the anomaly. To obtain a close fit between calculated and observed anomalies the body had to be slightly modified from the form indicated by the gravity data, and a possible solution is given in Fig. 43. It seems that the body must extend to great depth. Taking into account the complexity of the geology, complete accord of the two interpretations is unlikely; hence the interpretation can be regarded as satisfactory, although minor modifications to it may be necessary when more seismic work has been done. Geologically it seems reasonable.

Magnetic, gravity and seismic data therefore suggest that the northern margin of Bransfield Strait is a major fault or fault zone with an uplift of approximately 2 km. to the north.

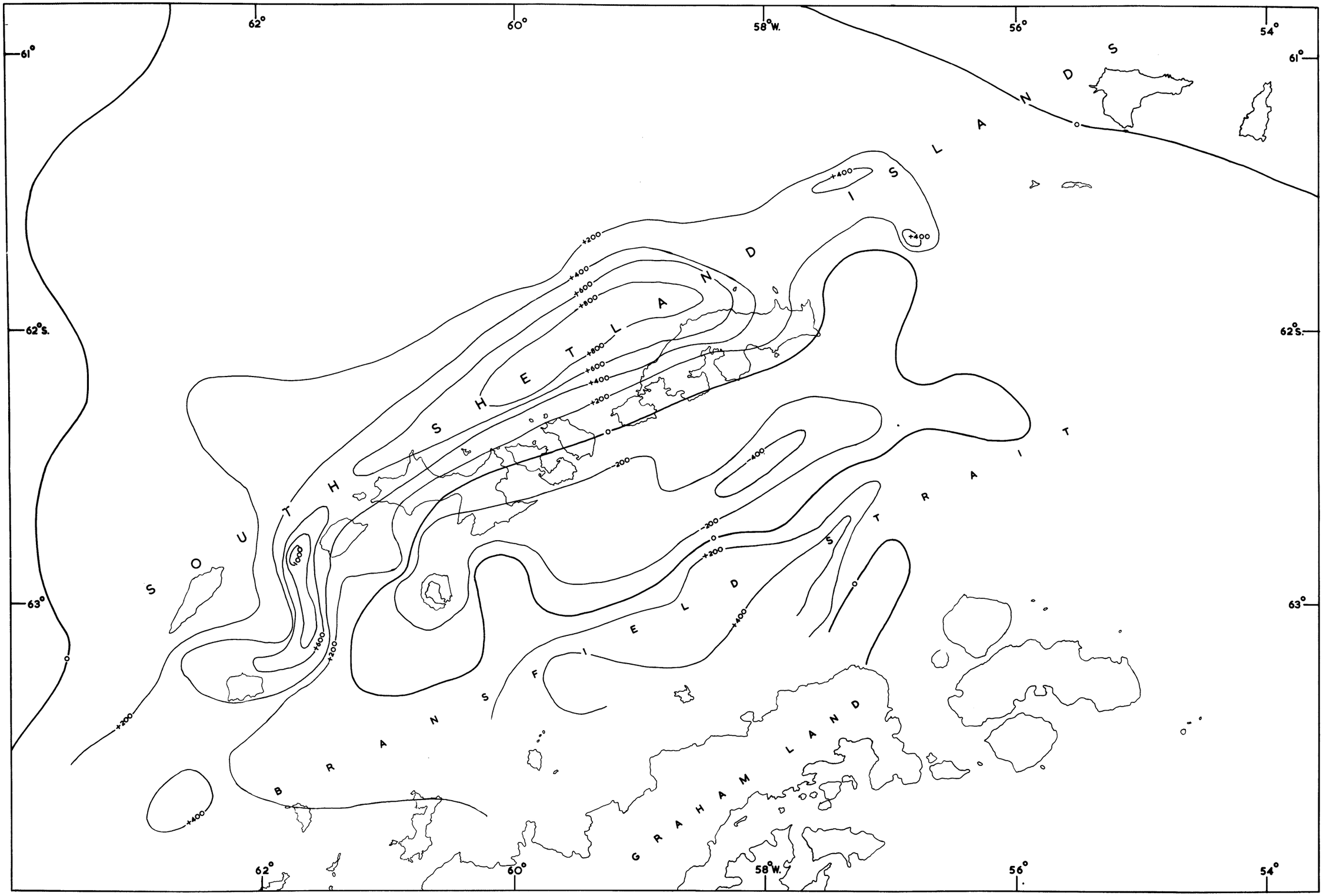

FIGURE 42

Map of the Bransfield Strait area showing total field magnetic anomalies in gamma after removal of the regional gradient.

IV. THE SEISMIC SURVEY

In the first season of seismic survey (1961–62) very simple equipment was used. An arrangement of four hydrophones was suspended at intervals of 200 ft. (61 m.) from a buoyant cable. The hydrophones were arranged to have neutral buoyancy and to float at a depth of about 100 ft. (30·5 m.). The output from each hydrophone was taken to a transistor amplifier; three of the channels had a response of about 5–100 c./sec. and they were used to detect the ground wave. The fourth channel had a higher frequency response and was specifically designed for receiving the water wave, though in practice it was found that this was adequately recorded on the other channels. A conventional galvanometer camera, loaned by the British Petroleum Co. Ltd., was used for recording. Shots were made up from naval demolition charges of T.N.T. and were electrically fired, the shot instant being relayed from H.M.S. *Protector* to R.R.S. *Shackleton* by radio. The noise level of the equipment was relatively high; it is thought this was partly due to unsatisfactory suspension of the hydrophones and partly due to ship noise. Using the maximum charge that could be reasonably handled (200 lb.; 91 kg.) restricted the range to about 15 miles (28 km.) even in fairly calm weather.

In the following season (1962–63) the amplifiers were replaced by a low-frequency, low-noise transistor amplifier system (GTR 200, Dresser Electronics, U.S.A.), and for convenience an ultra-violet paper recorder was used. An improved type of hydrophone suspension system was devised, but this did not reduce the noise level to as low a value as was hoped. It was found that in calm weather, using 300 lb. (136 kg.) T.N.T. depth charges, the maximum range that could be achieved was about 36 miles (67 km.). Fig. 44 shows the location of the seismic lines surveyed so far. The letter R against a line indicates that it has been shot from both ends.

The interpretation of the data has not yet been completed but a preliminary study has been made. The velocities given below are likely to be approximately correct but any depths and thicknesses quoted are only rough estimates.

The water depth in the area of the surveys to the north-east of Bransfield Strait varies between 0·7 and 1·8 km. Second arrivals on the travel time curve indicate the presence of an upper sediment layer with a velocity between 2·3 and 3·0 km./sec., extending down to a depth of 2 to 3 km. below sea-level. Below this are layers, well defined by first arrivals, having velocities varying between about 4·0 and 6·0 km./sec. The third and lowest layer reached in this region has its upper surface at a depth below sea-level of 4 to 6 km., and has a velocity between 7·0 and 7·5 km./sec. The existence of this high-velocity layer has been verified by subsequent work farther to the west.

On the ridge to the east of the South Orkney Islands there is a well-determined succession of three layers. There is a top layer of sediment which rests on a layer about 2 km. thick with a velocity of about 3·6 km./sec. Below this, at a depth of about 4 km., is the third layer having a velocity of about 5·8 km./sec. In the Scotia Sea, along the central part of the profile, the main crustal layer was observed to be at a depth of about 6 km. below sea-level and to have a velocity of about 6·0 km./sec. Some data indicate the presence of a higher-velocity layer underlying the 6·0 km./sec. crustal layer; however, this will not be commented on further until a more detailed analysis has been completed.

V. DISCUSSION OF RESULTS AND CONCLUSIONS

1. *Bransfield Strait*

In Bransfield Strait and the South Shetland Islands the general form of the gravity anomaly and the total magnetic field is now known, and a number of seismic refraction lines have been surveyed both along and across the Strait. Although most of the seismic measurements have still to be fully analysed, a tentative interpretation of the data has been made. It is believed that the South Shetland Islands are underlain at a comparatively shallow depth by very dense magnetic rocks having a high velocity, and thus probably of very basic composition. In fact, the material may well be intermediate in composition between that of the crust and the mantle.

It seems likely that the south-eastern margin of the South Shetland Islands is a major fault, for the gravity and magnetic anomalies are best fitted by assuming an uplift of the high-density rocks of some 2 km. to the north. There is also geological evidence of the existence of major faulting.

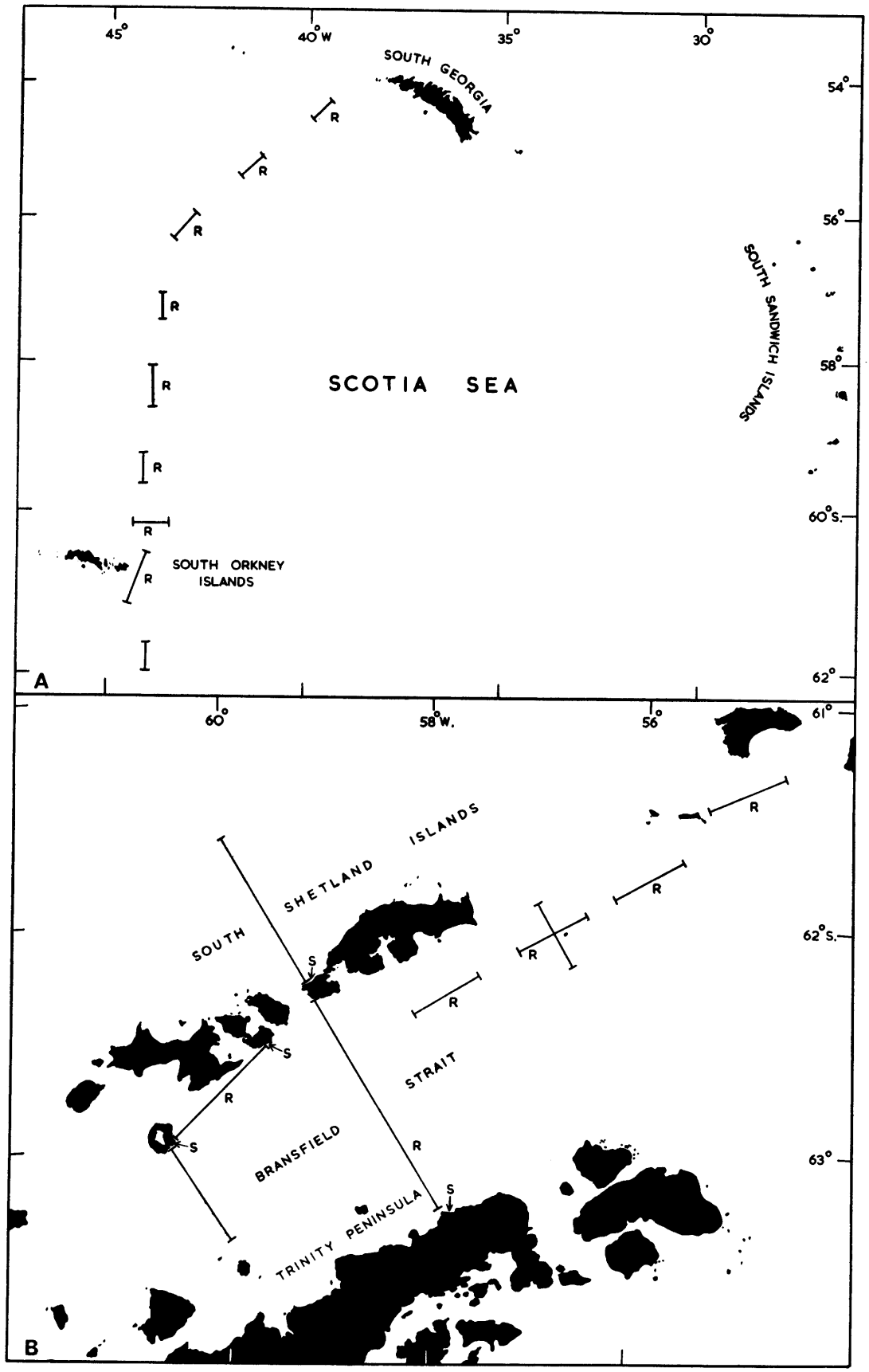

FIGURE 44

Seismic refraction lines surveyed in the 1961–62 and 1962–63 seasons:
A. Eastern Scotia Sea; B. Bransfield Strait area.
R. Reversed refraction line; S. Shore-based recording station.

Until the remainder of the seismic data has been interpreted it would not be helpful to discuss the structure of this region further, except to remark that there is at present no geophysical evidence of a similar fault on the opposite side of the Strait.

2. *Major features of the Scotia arc*

Considering the Scotia arc as a whole, one of the main features which emerges is the continuation of the submarine ridge from the Burdwood Bank to South Georgia as a non-magnetic structure. This would seem to imply that the rocks which produce strong magnetic anomalies to the north and south of the ridge are either non-existent or downwarped and deeply buried beneath non-magnetic sedimentary material. Seismic observations by J. and M. Ewing (1959) over the ridge to the south of the Falkland Islands indicate that the main crustal layer is depressed about 5 km. and that the bank is largely formed by a thick layer of consolidated sediments. By comparison with the geology of South America, these sediments can probably be assumed to be Cretaceous in age, but to have remained unaffected by Andean intrusion and metamorphism. The width of the ridge, as defined by the non-magnetic area, decreases towards South Georgia and there is a considerable thinning at about long. 45°W. Both this and a marked difference in the topography of the area east of this point suggest that a continuity of structure cannot be tacitly assumed to exist along the whole length of the ridge. It is also notable that so far no non-magnetic ridge of a similar character has been seen either east of South Georgia or on the southern side of the arc, although the considerable length of ridge between the South Sandwich and South Orkney Islands has not been surveyed.

The deep-water regions of the Scotia Sea have been subdivided into areas of different magnetic type and it has been suggested that the *B* type may be due to sub-sediment topography, either of lavas or of an "original" crust. Alternatively, it may be due to major basic intrusions rising almost to the ocean bottom. If this is so, over considerable areas the latter occur at fairly regular intervals of 10 to 20 miles (19 to 37 km.), and have a marked magnetic contrast with the surrounding rocks. Although intensity contrasts of the order required can be found within the observed range of basic rocks, the apparent contrast might well be increased between very similar petrographic types if they exhibited different polarization directions due to their different ages of formation. It should also be noted that intrusion on this scale probably implies a pre-existing state of tension within the intruded crust which may have had some relation to the movement of the adjacent continents. The structure of the crust in Drake Passage and the western part of the Scotia Sea north of about lat. 58°S. has been reported by J. and M. Ewing (1959) to be the same as the average Pacific Ocean basin structure. It consists of a thin layer of sediments, a layer of velocity 3·5 to 4·5 km./sec. and the main crustal layer with a velocity of 6·5 km./sec. Magnetically, this region is in general of *B* type, consisting of a series of anomalies several miles wide with an average amplitude of 150 gamma and spaced about 10 miles (19 km.) apart. They appear to originate at a shallower depth within the crust.

Although they are generally larger in amplitude (200–500 gamma) than the magnetic anomalies in Drake Passage, those observed by Mason and Raff (1961) in the eastern Pacific Ocean originate from a similar type of crust. They are also estimated to arise from sources at no great depth beneath the sea bottom and are orientated parallel to the dominant structural trend.

Heezen (1962) has reported the results of geophysical measurements from abyssal hill and plain areas in the Atlantic Ocean. The crustal sections quoted are almost identical to that reported by Ewing in Drake Passage, and he considers that it is evident from gravity, magnetic and seismic profiler results that the upper surface of the 4·5 km./sec. layer has a considerable topography that is generally buried beneath the abyssal plains and exposed on the abyssal hills. This layer is also observed over oceanic rises and ridges where it gives rise to regular series of magnetic anomalies (Heezen, Tharp and Ewing, 1959). From specimens obtained by dredging, Heezen has suggested that it is predominantly altered igneous rock.

It would be interesting to know whether these oceanic Pacific and Atlantic areas are in fact of *B* type. Should they prove to be so, and thus similar to those of the Drake Passage area, it would suggest that the existence of a *B* magnetic type is an indicator of oceanic crust. The existence of a *B* type area over the abyssal hills region in the Atlantic Ocean would also strongly support the suggestion advanced on p. 30 that magnetic features of this type may well be due mainly to the topography of the surface of the crystalline crustal layers.

The seismic results reported on p. 39 are largely from an area due north of the South Orkney Islands, where few magnetic measurements were made prior to 1962. However, a preliminary examination of the measurements made in the 1962–63 season (not shown on the map), taken in conjunction with those obtained earlier, indicates that the area may be of somewhat different magnetic character from that in Drake Passage discussed above.

The seismic results also indicate a crustal structure which is different from that in Drake Passage, and which is notable for the presence of a low crustal velocity of about 6 km./sec. In this respect the crust is similar to that of the Venezuelan basin, where a similar velocity for the main crustal layer has been reported (Officer and others, 1959). According to Affleck (1948), in this area there are a series of magnetic anomalies of approximately 20 miles (37 km.) wave-length, and with an amplitude of 100–200 gamma at sea-level. These are calculated to arise from sources near the sea bottom.

The presence of a region in the Scotia Sea with a crust which may be of mixed type raises the problem, already discussed by Officer in connection with the Caribbean data, as to whether this is relic or potential continental crust. This is a problem that at the present time has not been resolved. Thus, although the possible presence of a crust of this type lends some support to the geological speculations of both Hawkes and Matthews mentioned on p. 3, the extent and boundaries of the different types of crust will have to be determined before any definite conclusions can be reached about the history of this region.

VI. ACKNOWLEDGEMENTS

THE authors wish to thank Sir Vivian Fuchs, Director of the British Antarctic Survey, for providing extensive facilities that enabled the field work to be carried out. The helpful co-operation of Captain D. Turnbull (R.R.S. *Shackleton*), Captain R. H. Graham, M.V.O., D.S.C., R.N. (H.M.S. *Protector*) and Captain W. Johnston (R.R.S. *John Biscoe*) throughout the period of the surveys is gratefully acknowledged. Professor F. W. Shotton kindly made available laboratory facilities in the Department of Geology, University of Birmingham. Mr. H. E. Chapman kindly drew the maps.

VII. REFERENCES

ADIE, R. J. 1957*a*. Geological Research in Graham Land. *Advanc. Sci., Lond.*, No. 53, 454–60.

———. 1957*b*. Geological Investigations in the Falkland Islands Dependencies before 1940. *Polar Rec.*, **8**, No. 57, 502–13.

———. 1958. Geological Investigations in the Falkland Islands Dependencies since 1940. *Polar Rec.*, **9**, No. 58, 3–17.

———. 1962. The Geology of Antarctica. (*In* WEXLER, H., RUBIN, M. J. *and* J. E. CASKEY, *ed. Antarctic Research: the Matthew Fontaine Maury Memorial Symposium.* Washington, D.C., American Geophysical Union, 26–39.) [Geophysical Monograph No. 7.]

———. 1964. Geological History. (*In* PRIESTLEY, R. E., ADIE, R. J. *and* G. DE Q. ROBIN, *ed. Antarctic Research.* London, Butterworth and Co. (Publishers) Ltd., 118–62.)

AFFLECK, J. 1948. Aeromagnetometer Profile Flown from Venezuela to Texas. *World Oil*, July, Sect. 1, 223–24, 227–28.

BARTH, T. F. W. *and* P. HOLMSEN. 1939. Rocks from the Antarctandes and the Southern Antilles. Being a Description of Rock Samples Collected by Olaf Holtedahl 1927–1928, and a Discussion of Their Mode of Origin. *Sci. Res. Norweg. antarct. Exped.*, No. 18, 64 pp.

BLUNDELL, D. J. *and* P. J. STEPHENSON. 1959. Palaeomagnetism of Some Dolerite Intrusions from the Theron Mountains and Whichaway Nunataks, Antarctica. *Nature, Lond.*, **184**, No. 4702, 1860.

BUNCE, E. T. *and* D. A. FAHLQUIST. 1962. Geophysical Investigation of the Puerto Rico Trench and Outer Ridge. *J. geophys. Res.*, **67**, No. 10, 3955–72.

COHEN, T. J. 1963. Gravity Survey of Chilean Antarctic Bases. *J. geophys. Res.*, **68**, No. 1, 263–66.

EWING, J. *and* M. EWING. 1959. Seismic Refraction Measurements in the Scotia Sea and South Sandwich Island Arc. (*In* SEARS, M., *ed. International Oceanographic Congress Preprints.* Washington, D.C., American Association for the Advancement of Science, 22–23.)

EWING, M. *and* L. ENGEL. 1962. Seismic Shooting at Sea. *Sci. Amer.*, **206**, No. 5, 116–24, 126.

GRIFFITHS, D. H. 1963. Geophysical Investigations in the Scotia Arc and Graham Land. *British Antarctic Survey Bulletin*, No. 1, 27–32.

——— *and* R. P. RIDDIHOUGH. 1963. Correlation of Widely Spaced Magnetic Profiles in Oceanic Areas. *Nature, Lond.*, **199**, No. 4890, 251–53.

HAWKES, D. D. 1962. The Structure of the Scotia Arc. *Geol. Mag.*, **99**, No. 1, 85–91.

HEEZEN, B. C. 1962. The Deep-sea Floor. (*In* RUNCORN, S. K., *ed. Continental Drift.* New York and London, Academic Press, 235–88.) [International Geophysics Series, Vol 3.]

———, THARP, M. *and* M. EWING. 1959. The Floors of the Oceans: I. The North Atlantic. *Spec. Pap. geol. Soc. Amer.*, No. 65, 122 pp.

HOLTEDAHL, O. 1929. On the Geology and Physiography of Some Antarctic and Sub-Antarctic Islands. *Sci. Res. Norweg. antarct. Exped.*, No. 3, 172 pp.

MASON, R. G. 1960. Geophysical Investigations of the Sea Floor. *Lpool Manchr. geol. J.*, **2**, Pt. 3, 389–410.

——— *and* A. D. RAFF. 1961. Magnetic Survey off the West Coast of North America, 32°N. Latitude to 42°N. Latitude. *Geol. Soc. Amer. Bull.*, **72**, No. 8, 1259–65.

MATTHEWS, D. H. 1959. Aspects of the Geology of the Scotia Arc. *Geol. Mag.*, **96**, No. 6, 425–41.

OFFICER, C. B., EWING, J. I., HENNION, J. F., HARKRIDER, D. G. *and* D. E. MILLER. 1959. Geophysical Investigations in the Eastern Caribbean: Summary of 1955 and 1956 Cruises. (*In* AHRENS, L. H., PRESS, F., RANKAMA, K. *and* S. K. RUNCORN, *ed. Physics and Chemistry of the Earth*, **3**. London, New York and Paris, Pergamon Press, 17–109.)

PETERS, L. J. 1949. The Direct Approach to Magnetic Interpretation and Its Practical Application. *Geophysics*, **14**, No. 3, 290–320.

TYRRELL, G. W. 1945. Report on Rocks from West Antarctica and the Scotia Arc. '*Discovery*' *Rep.*, **23**, 37–102.

WILSON, J. T. 1954. The Development and Structure of the Crust. (*In* KUIPER, G. P., *ed. The Solar System: II. The Earth as a Planet.* Chicago, University of Chicago Press, 138–214.)

WOOLLARD, G. P. 1960. Seismic Crustal Studies during the IGY. Part I: Marine Program. *Trans. Amer. geophys. Un.*, **41**, No. 1, 107–13. [*I.G.Y. Bull.*, No. 33, 107–13.]

——— *and* W. E. STRANGE. 1962. Gravity Anomalies and the Crust of the Earth in the Pacific Basin. (*In* MACDONALD, G. A. *and* H. KUNO, *ed. The Crust of the Pacific Basin.* Washington, D.C., American Geophysical Union, 60–80.) [Geophysical Monograph No. 6.]

WORZEL, J. L. *and* G. L. SHURBET. 1955. Gravity Interpretations from Standard Oceanic and Continental Crustal Sections. (*In* POLDERVAART, A., *ed.* Crust of the Earth. *Spec. Pap. geol. Soc. Amer.*, No. 62, 87–100.)

ZHIVAGO, A. V. 1962. Outlines of Southern Ocean Geomorphology. (*In* WEXLER, H., RUBIN, M. J. *and* J. E. CASKEY, *ed. Antarctic Research: the Matthew Fontaine Maury Memorial Symposium.* Washington, D.C., American Geophysical Union, 74–80.) [Geophysical Monograph No. 7.]